Letter to reviewers

Dear Editor,

please find below our answers to the reviewers' comments.
In the new version of the manuscript we carefully revised all the figures and the typesetting of the equations, variables and pieces of code (as recommended by Rev#2). The abstract, the introduction and the discussion have been modified according to the suggestions of Rev#2. Finally, we also provided the missing technical information and we amended the scientific description of some topics, which was rather imprecise (as pointed out by Rev#1).

In the response letter, the comments of the reviewers are in *ITALIC SMALL CAPITAL* whereas author's responses are in upright font. A revised manuscript has also been uploaded. We provided a marked-up version of the manuscript showing the changes we made (we used the track changes in Word).
We hope that the revision will meet the high standards of Geoscientific Model Development publications.

Best regards,

Gianpiero Cossarini and co-authors

REVIEWER #1

1.1 GENERAL REMARKS

THIS MANUSCRIPT PRESENTS A SOFTWARE INTERFACE THAT LINKS TWO WELL ESTABLISHED MODELS WITHIN THE MARINE SCIENCE COMMUNITY FOR OCEAN CIRCULATION AND MARINE BIOGEOCHEM-ISTRY, PROVIDING A NEW VALUABLE TOOL FOR A VAST RANGE OF APPLICATIONS INDICATED IN THE WORK. I'D LIKE TO COMPLIMENT THE AUTHORS FOR THEIR EFFORT IN COVERING THE WIDE RANGE ARGUMENTS INVOLVED IN DESCRIBING A COUPLED HYDRODYNAMIC BIOGEOCHEMICAL SYSTEM COMPREHENSIV- LEY IN A REASONABLE AMOUNT OF SPACE WITH AN ADEQUATE LEVEL OF DETAIL WITHOUT ANY MAJOR OMISSION. THE WORK COVERS ALL RELEVANT SCIENTIFIC AND TECHNICAL ASPECTS AND IS THEREFORE CERTAINLY ELIGIBLE FOR PUBLICATION IN GEOSCIENTIFIC MODEL DEVELOPMENT AFTER THAT SOME MINOR ISSUES HAVE BEEN ADDRESSED WHICH CONCERN SOME MISSING TECHNICAL INFORMATION AND INPRECSIONS IN THE SCIENTIFIC DESCRIPTION, THAT ARE GIVEN BELOW.

We thank the reviewer for the positive comment. We improved the quality of the manuscript incorporating all the missing information and the corrections suggested by the reviewer.

1.2 TECHNICAL OMISSIONS

IN ORDER TO BENEFIT USERS OF THIS SOFTWARE INTERFACE, I BELIEVE THE ADDITION OF THE FOLLOWING INFORMATIONS WOULD BE CRUCIAL:THE VERSION OF THE MITGCM USED IN THIS WORK HAS BEEN SPECIFIED, BUT AN INDICATION OF WHERE TO RETRIEVE THE MODEL CODE FROM WOULD BE HELPFUL. OF COURSE, NOT BEING THE DEVELOPERS THEMSELVES, THE AUTHORS WILL HAVE NO CONTROL OF THE FUTURE ACCESSIBILITY TO THE POINT OF RETRIEVAL, BUT AT LEAST AN INDICATION OF WHERE OR HOW TO OBTAIN THE CODE AT PRESENT IS REQUIRED.

That information was missing: we specified the MITgcm website and the two possible ways to obtain the code in P6L7-12 The link to download the TAR file (http://mitgcm.org/download/) and the link to the CVS pserver (http://mitgcm.org/public/using_cvs.html) can be accessed very easily from the MITgcm home, so we don't think it is worth specifying them in the text. Similarly for the terms TAR and CVS, which are quite common in the modeling community and which we don't think that should be explained.

WHAT IS THE PRECISE VERSION OF THE BFM CODE, THAT WAS USED? I GATHER THE MODEL IS DISTRIBUTED VIA GIT, SO A COMMIT HASH AND THE LINK TO THE REPOSITORY WOULD SUFFICE.

The current coupling uses the BFM version v2, which was used in several papers describing the biogeochemistry of the Mediterranean Sea (Lazzari et al.,2012, 2016; Teruzzi et al., 2013; Cossarini et al., 2015; Melaku Canu et al., 2015).
As we explain in the text, the BFM can be downloaded by registering and requesting the code through the BFM website (http://bfm-community.eu).
The text has been modified as follows: "For this application, we adopted the configuration version v2 (Lazzari et al. 2012, 2016; Teruzzi et al., 2013, Melaku Canu et al., 2015, Cossarini et al., 2015b), which can be downloaded upon request from the BFM-consortium.eu website " at P7L31-32.

PROGRAMMING LANGUAGES AND VERSION OF ALL PARTS SHOULD BE SPECIFIED. TO MY UNDERSTANDING ALL THREE ARE CODED IN FORTRAN, BUT ONLY FOR THE BFM THIS IS CLEARLY STATED INCLUDING THE FORTRAN VERSION.
We specified that MITgcm is a modular Fortran77 code in P6L9, and that BFM is Fortran90 code in P7L14.

AS I ASSUME DEVELPOMENT OF THE COUPLE WILL CONTINUE, ALSO A HASH FOR THE COUPLER LIBRARY IS NEEDED.
Yes, this is the first release of the `BFMCOUPLER` package and its development will continue. It has been named v1.0. The version is added `BFMCOUPLER` in the title of the manuscript, in the Appendix at P23L6 and L11 and P26L11 and in the headers of all `BFMCOUPLER` files available in the GitHub repository.

SPECIFICATIONS OF INPUT/OUTPUT FORMATS ARE MISSING.
Input/output of the coupled model is based on the native MITgcm I/O package (`MDSIO`), which is a package that contains a group of Fortran routines for reading and writing direct-access binary files.
A sentence has been added in the description of the `BFMCOUPLER` package in the Appendix A at P24L21-22: "Input/output directives are based on the native MITgcm I/O package (`MDSIO),` a set of Fortran routines for reading and writing direct-access binary files".

1.3 DETAILED COMMENTS

PAGE 2, LINE 12: CHECK AUTHOR NAMES AND PUBLICATION YEAR.
Butenschön et al., 2016 has been corrected

PAGE 2, LINE 15: I DON'T THINK IT'S A MATTER OF COMPLEXITY, BUT A STRUCTURAL ARGUMENT THAT DICTATES THE MODEL HIERARCHY BETWEEN PHYSICAL DRIVER AND BIOGEOCHEMICAL MODEL: IN ALL CITED CASES AND ALL OTHER COUPLINGS I AM AWARE OF, THE PHYSCIAL MODEL PRO- VIDES THE OVERARCHING GEOMETRICAL STRUCTURE OF THE MODEL (AND CAN RUN ON ITS OWN), WHILE THE BIOGEOCHEMICAL MODEL TYPICALLY JUST COMPUTES BIOGEOCHEMICAL RATES ON A PER PIXEL BASE AND AT THE BARE MINIMUM REQUIRES A 0D DRIVER TO RUN ANY SIMULA- TION. IN FACT, I DON'T THINK THAT THE STATEMENT THAT THE PHYSICAL MODELS ARE FAR MORE COMPLEX HOLDS GENERALLY.
The reviewer is right: the sentence is rather misleading. Please see also Rev#2's comments about this issue (P2L15F of Rev#2). The sentence has been corrected as follows: " … , in general, hydrodynamic models have been already developed to solve the partial differential equation of tracers and provide the coding infrastructure to handle the spatial-temporal properties of the simulations (i.e. bathymetry, boundaries, computational domain discretization) " at P2L25-27.

PAGE 2, LINE 18: INSTEAD OF "INPUT/OUTPUT DIRECTIVES" I'D PREFER INTERFACE SPECIFICATIONS OR IF YOU WANT MORE USE THE TECHNICAL TERM APPLICATION PROGRAMMING INTERFACES (APIS) IN ORDER TO NOT CONFUSE WITH ACTUAL MODEL IN- AND OUTPUT DATA.
Thank you for the suggestion: the term "application programming interfaces (APIs)" has been used instead of "input/output directives" at P2L29, P8L8, P23L10.

PAGE 2, LINE 32-34: THE CHOICE OF THE AUTHORS IN ITSELF DOESN'T REQUIRE JUSTIFICATION, BUT IS THERE ANY EVIDENCE THAT PERFORMANCE WOULD SUFFER FROM USING THESE TOOLS? I WOULD HAVE THOUGHT THAT DEPENDS (TO SOME DEGREE) ON HOW WELL THEY ARE WRITTEN?
This part of the introduction has been significantly revised considering also the comments of Rev#2.
In the revised text, we explain the motivations for our online coupling (i.e., capability to drive the biogeochemistry at the same frequency of the hydrodynamic processes, to avoid the use of large files in which to save hydrodynamic variables at high frequency, to ensure the use of consistent differential operators - advection and diffusion - for hydrodynamics and biogeochemistry and to describe possible feedbacks from biogeochemistry to hydrodynamics). We removed the conjectures regarding other couplers.

PAGE 2, LINES 34-38: WORTH MENTIONING HERE IF IT DEALS WITH ONLINE, OFFLINE COUPLING OR BOTH.
"Online" is added at P3L16.

PAGE 4, LINE 36: ANY EXPLICIT TIME INTEGRATION METHOD IS FORWARD-IN-TIME, THAT INCLUDES ADAMS-BASHFORTH SCHEMES. WHICH ONE IS USED HERE, EULER FORWARD?

Yes. We specified Euler "forward-in-time" in P6L22 and L28, and also "backward" in P6L21.

EQUATION 10: THE MEANING OF THE HERETO UNUSED VARIABLES NEEDS TO BE SPECIFIED. SPECIFICALLY THE MEANING OF THE TWO DIFFUSION TERMS SHOULD BE MADE CLEAR. ALSO, AS THESE EQUATIONS ARE STILL GENERIC AT THIS POINT, IT MAY BE WORTH USING A DIFFERENT SUB-SCRIPT FOR THE BIOGEOCHEMICAL SOURCES AND SINKS.

We agree with the reviewer. Equation (10) has been corrected by substituting $\mathbf{R}_{BFM}$ with $\mathbf{R}_{bio}$, which is first introduced in equation (7) and named at P5L5. Further, the two diffusion terms of equation (10) have been explained in the sentence: "The first three …, where K_H and K_V are the horizontal and vertical diffusivities, respectively, which are considered separately because they have different spatial scales." at P5L15-16.

PAGE 4, LINES 9-15: MIGHT BE WORTH ALSO TO REFER ALREADY TO THE POSSIBILITY OF SURFACE/BOTTOM BOUNDARY CONDITIONS FOR THE BIOGEOCHEMISTRY INTRODUCED IN THE BFMCOUPLER SECTION LATER.

We agree to introduce here the surface and bottom forcing and we modified the sentence as follows: "The other components, such as Eq. (8), the biogeochemical tracers forcing terms ($\mathbf{Q_c}$ e.g. surface and bottom boundary conditions) and the sinking terms, can be handled by both the hydrodynamic and biogeochemical models" at P5L20-21. However, since this is still a general description, we would prefer to postpone to the section dedicated to the coupler (section 2.4) the description of the components and processes that are handled directly by the coupler.

PAGE 6, LINES 16-17: THE INFORMATION FLOW BETWEEN BFM, MITGCM AND THE COUPLER IN BE- TWEEN IS NOT ONE-WAY AS CLEARLY INDICATED BY FIGURE 2 AND THE FOLLOWING TEXT. IT IS TRUE THAT THE OCEAN PHYSICS IN THE DESCRIBED SETTING REMAIN UNAFFECTED BY THE BIOGEOCHEMISTRY, BUT THAT DOESN'T MEAN THAT THE INFORMATION FLOW IS ONE-WAY, AS THE TRANSPORT MODEL FOR PASSIVE TRACERS SITS IN THE MITGCM CODE AND REQUIRES THE BIOGEOCHEMICAL SOURCES AND SINKS FOR INTEGRATION (AND BIOGEOCHEMICAL VERTICAL MOVEMENT).

We agree, "one way" has been removed and the sentence has been rephrased as follows: "As an interface, the `BFMCOUPLER` manages the transfer of information that is required by the BFM from both the hydrodynamic and transport sub-models of the MITgcm, and provides the integration solver (a MITgcm package) with the biogeochemical surface and bottom forcing and the sink/sources terms originated from the BFM ($gTracer_{bio}$)." at P8L25-26.

PAGE 6, LINE 33: "A SOURCE SPLITTING SCHEME IS ADOPTED": THE INSERTION OF THE BIOGEOCHEMICAL RATES INTO THE TRANSPORT SOLVER CONSTITUTES A SOURCE SPLITTING ONLY OF THE INTEGRATION SCHEME APLLIED EFFECTIVELY OMITS INFORMATION OR INTERMEDIATE STEPS THAT ARE REQUIRED BY THE COUPLER. IN PARTICULAR, IF THE INTEGRATION SCHEME IS A SIMPLE EULER FORWARD SCHEME, THE INSERTION OF THE BIOGEOCHEMICAL RATES DOES NOT INVOLVE ANY FORM OF SPLITTING, BUT CONSTITUTES A DIRECT INTEGRATION OF THE TERMS IN EQUATION 10.

We agree with the reviewer, the use of the term "source splitting scheme" is misleading. We intended a source splitting scheme with synchronous time steps, that was then compared to the operator splitting scheme with different time steps. However, we agree that the term source splitting, as described in the original paper, is misleading. Therefore we decided to substitute "source splitting" with "direct integration scheme" throughtout the text.

PAGE 7, LINES 23-24: THE OPTION OF APPLYING DIFFERENT TIME STEPS TO THE TWO MODES IS NOT UNIQUE TO THE PROCESS SPLITTING, BUT CAN BE EASILY ADOPTED IN THE SOURCE SPLITING METHOD BY UPDATING THE RATES OF THE SLOWER PROCESS ONLY ON INTERMEDIATE TIME STEPS. (E.G. BLOM, J.G., VERWER, J.G., 2000. A COMPARISON OF INTEGRATION METH- ODS FOR ATMOSPHERIC TRANSPORT-CHEMISTRY PROBLEMS. JOURNAL OF COMPUTATIONAL AND APPLIED MATHEMATICS 126, 381–396. DOI:10.1016/S0377-0427(99)00366-0)

As explained at the previous point, the term "source splitting" has been dropped. We agree with reviewer's comment and, in order to be more clear, we referred to "direct integration" instead of "source splitting".

PAGE 7, LINE 26-27: "TO INCREASE THE COMPUTATIONAL PERFORMANCE OF THE ENTIRE CODE" IN WHICH WAY?
We inteded the overall time required to perform a coupled simulation. The sentence has been changed as follows: "A third option is a operator splitting algorithm, which involves the MITgcm package LONGSTEP (Adcroft et al., 2016) and adopts different time steps for the hydrodynamic and transport-biogeochemical components, thus increasing the computational performance of a coupled simulation" at P10L12-14.

PAGE 8, LINE 15 FF, EQ 14: WHAT WOULD ACTUALLY BE REQUIRED IS THE AVERAGE LIGHT IN EACH CELL, WHICH GIVEN THE EXPONENTIAL DISTRIBUTION IS NOT THE LIGHT IN THE CELL CENTRE. USING THE SAME FORMULA, IT IS STRAIGHT FORWARD TO COMPUTE THE INTEGRAL OF LIGHT BETWEEN THE UPPER AND LOWER CELL FACE AND DIVIDE BY THE CELL THICKNESS IN ORDER TO ARRIVE AT THE CORRECT NUMBER.
The current version of the BFM model (version v2, which is used for Mediterranean Sea simulations) was calibrated (i.e., parameters of the phytoplankton growth formulation) to use the light at the center of the cell (Lazzari et al., 2012, 2016). As we described in the revised section 2.3 (P7L29-31) we specify that we use the v2 configuration of the BFM model, which is fully described in the aforementioned papers. The light formulation is consistent with the BFM model implementation, however, we agree that it is easy to accomplish the implementation of alternative light locations (i.e., average light in the cell or light at the top of the cell). Finally, considering the fine discretization of the vertical dimension (cell thickness lower than 5 m down to 45 m and lower than 10 m down to 120 m), the differences between PAR at center of the cell and integral PAR of the cell are quite low (less than 6% down to 45 m and less than 11% down to 130 m).

PAGE 8, EQ. 15: HOW IS THIS PDE SOLVED NUMERICALLY? PROVIDE THE SCHEME OR A REFERENCE TO A FULL DESCRITION.
The sinking is solved numerically based on an Euler forward scheme. This is added to the text at P12L2-3.

PAGE 9, LINE 5: WHAT HAPPENS TO SINKING PHYTOPLANKTON THAT HITS THE SEA FLOOR?
The solution of the sinking equation (Eq. 15) has a boundary at the last cell of the water column. There is no sinking flux from the last cell to the sea bottom. However, in order to avoid misunderstandings, we have substituted the word "sink out" with "is exported out from" in the sentence that describes the burial process at P12L16. In the case of burial, it is assumed that a fraction of the detritus concentration (but not of the phytoplankton) of the last cell of the water column hits the sea floor and exits from water column.

PAGE 9, LINE 28: ". . . WHICH ARE . . . "
Done. P13L11

PAGE 10, LINE 6: FURTHER DOWN IT APPEARS THAT AT LEAST THE SURFACE HEAT HAS A SEASONAL CYCLE, SO IS NOT STEADY?
Yes, surface heat and mass fluxes have a seasonal cycle, the adjective "steady" is referred to wind only. The sentence has been made clearer as follows: "… forced by steady winds and a seasonal cycle of surface heat (downward long-wave and short-wave radiation) and mass (precipitation) fluxes" at P13L27
Further, in Appendix A at P26L9-10, the sentence that describes the idealized case, which can be downloaded along with the code, has been corrected as well.

PAGE 11, LINE 6: "THE LIGHT EXTINCTION FACTOR WAS CALCULATED CONSIDERING A BACKGROUND VALUE".
Done: "s" has been removed. Further, the value of the background extinction factor has been added as follows: "… considering a background value (K_{ext}=0.035 m^{-1}) …" at line P15L3.

PAGE 11, LINE 26: WELL-LIGHTED -> WELL-LID
Done.

FIGURE 6: CAPTION: WHAT IS LSN?

LS_n is the number of ocean dynamics time steps performed within a single ptracer step. The explanation of LS_n has been introduced in the text at P10L14 and reported in the caption of Figure 6 for sake of clarity.

PAGE 11, LINE 33-34: "... TO SOLVE ... "
Done. P15L31

PAGE 11, LINE 36: HOW DOES THE SCALING WITH NUMBERS OF TRACERS EMERGE FROM THE FIGURE? WHAT EXPERIMENTS WERE DONE IN REGARD?
We performed four tests using the PTRACER package without the biogeochemical component and varying the number of passive tracers (10, 20, 40 and 51). We decided not to show these results, which prove that the computation cost increases almost linearly with the number of the passive tracers, because we thought they were quite "trivial" and predictable. Further, an indirect proof of this result is also shown in Figure 6. The solution of temperature and salinity equations (i.e., the transport of two tracers) requires almost 390 s, whereas the solution of transport of the 51 biological tracers requires about 9000 s. So, the transport of each tracer is solved in almost 190-200 s, and the computational cost increases roughly with the number of the tracers.
We have added the following "(e.g., $Tracers_{trsp}$ is almost 25 times larger than the time used to solve for temperature and salinity; Fig. 6)" in the text at P16L2-3.

PAGE 11, LINE 40: 2400S = 40' NOT 45'? WHAT DOES LSN MEAN, I SUPPOSE NUMBER OF TIME STEPS PER LONG STEP, BUT SHOULD BE SPECIFIED.
Done: LS_n is now first introduced at P10L15; and the sentence has been rewritten as follows "With a LS_n sets to 8 (a time step for tracers, Δt_{trc} , equals to 2400 s), the …" at P16L7.

FIGURE 7: ETA?
Eta has been substituted with Sea Surface Height (SSH).

PAGE 12, LINE 36: CONNECTED TO THE IONIAN SEA RATHER THAN THE EASTERN MED.
Done. Ionian Sea instead of Eastern Mediterranean Sea at P17L12.

PAGE 13, LINE 12: DAILY FRESH WATER FLOW RATE
Done. "fresh water" has been added at P17L28.

PAGE 13, LINE 35: IS THE BULK BACKGROUND EXTINCTION COEFFICIENT ADEQUATE CONSIDERING THE AMOUNT OF GELBSTOFF IN THE NORTHERN ADRIATIC?
Background extinction coefficient has been set considering a longitudinal gradient, according to the results presented in Lazzari et al., 2012. The sentence, which erroneously reported a constant background extinction coefficient, has been changed as follows "The background water light extinction coefficient was set considering a longitudinal negative gradient according to Lazzari et al. (2012)" at P18L20.
In any case, we think that the study of the effect of riverine yellow-substances on the water transparency in the northern Adriatic Sea would require a dedicated investigation, which should simulate the dynamical evolution of a new state variable for the terrestrial detritus concentration (yellow substance). An alternative solution would be the use of satellite maps of Kd as background extinction coefficient. In both cases, the coupled model has all the elements in order to carry out such an investigation.

PAGE 14, LINES7-9: THE LARGE SCALE OSCILLATIONS INDICATE INSTABILITY RATHER THAN INACCURACY WHICH MAY HAVE INCREASED EARLIER, CONSIDERING THAT THE DOMINANT TIME SCALES WILL BE DIFFERENT WITH RESPECT TO THE GYRE CONFIGURATION. OR HAVE YOU ACTUALLY ASSESSED THE INACCURACY?
The accuracy has been computed as the annual average of the root mean square of the differences of the weekly 3D fields between the reference solution ($LS_n = 1$) and the solution obtained when LS_n equals 3, 6, 9 and 12. This has been explained in the caption of Table 2.

The sentence has been simplified, avoiding comments on results which are not shown: "Then, time steps higher than 30 minutes substantially decreased the accuracy, without further reducing the computational cost (Table 2)" at P19L1-2.

PAGE 13, LINE 39: NO BENTHIC CLOSURE AS DESCRIBED PREVIOUSLY?

Yes, the set up of the Adriatic-Ionian model doesn't have bottom forcing because very few information are available on bottom fluxes and their temporal and spatial variability in the study area. We think that the investigation of the bottom-water column interaction effects would deserve a dedicated investigation, since it can have important effects on the productivity in the shallow continental shelf areas. A comment about the importance of coupling the present model with a benthic sub-model is present in the discussion section. Thus, we mostly focused our presentation on the results of the pelagic area (e.g., Figure10: vertical structure of variables in open sea points; Figure 11: transport of carbon across the Otranto strait).

PAGE 14 LINE 33: MUCH LOWER MIXED LAYER DEPTH IN WINTER FIGURE 10: MENTION THAT PHOSPHATE IS IN CONTOURS.

Done; then, Figure 10 has been redrawn considering also the comments of Rev#2.

PAGE 14, LINE 39: "SUPERIMPOSED LONGITUDINAL GRADIENT OF THE BACKGROUND LIGHT EXTINCTION": THIS IS IN CONTRAST TO THE CONFIGURATION DESCRIPTION IN LINE 35 OF PAGE 13 WHICH MENTIONS A CONSTANT BACKGROUND EXTINCITION.

As described at the point *PAGE 13, LINE 35*, the background extinction coefficient has been set considering a longitudinal gradient, according to the results presented in Lazzari et al., 2012. The sentence, which erroneously reported a constant background extinction coefficient, has been changed as follows "The background water light extinction coefficient was set considering a longitudinal negative gradient according to Lazzari et al. (2012)" at P18L20.

PAGE 15, LINE 1: CONSISTENT

Done.

PAGE 15, LINE 16-17: DROP "INTO THE MEDITERRANEAN SEA"

We would prefer to leave the term "into the interior of the Mediterranean Sea", because the net transport of carbon through the Otranto strait from the Adriatic occurs at the deeper layers. Thus, we would like to convey the message that the carbon is then entrapped in the deep water masses of the Mediterranean Sea.

PAGE 15/16, LINE 39-2: A STRING MATCHING MECHANISM USING VARIABLE METADATA WOULD BE MORE TRANSPARENT.

To our understanding, this would necessitate the use of pointers that systematically link the MITgcm ptracers to the BFM variables for the formulations used in the `BFMCOUPLER`. This could result in an increase of the complexity of the coding. The actual programming effort to link BFM variables and MITgcm tracers is quite small. Indeed, the list and order of the BFM variables are described only once in the include files `BFMCOUPLER_VARS.h` and `BFM_var_list.h`; and in the input file `data.ptracer`.

PAGE 16, LINE 4-5: EFFICIENCY IN SPATIAL DOMAIN DECOMPOSITION PARALLELISATION IS ALSO CONSIDERED IN OTHER COUPLING INTERFACES INCLUDING THE ONES CITED, SO NOT UNIQUE TO THIS INTERFACE. IT MAY BE MORE EFFICIENT, BUT THAT STATEMENT REQUIRES EVIDENCE.

We agree with the reviewer, this sentence was not clear (see also Rev#2 on this issue). We wanted to state that the efficiency of a coupled code can be an issue. Our coupling (as others like FABM and MESSy) is capable to handle to this aspect.

The sentence has been rewritten as follows: "Despite the growth of computational resources, the efficiency of coupled codes can be still an issue because of the large size of the computational grids (Blom and Verwer, 2000). Domain decomposition and parallelization tools are available in several coupling environments (e.g., FABM, Bruggeman and Bolding, 2014; and MESSy, Jöckel et al., 2008). Likewise, our coupling scheme has been thought to fully exploit the parallelization efficiency of the MITgcm (Marshall et al., 1997), and no additional coding effort (in terms of parallelization) is required by the users" at P21L13-17.

REVIEWER # 2

IN THEIR MANUSCRIPT, THE AUTHORS PRESENT A NEW MODULAR COUPLING SCHEME BETWEEN THE MIT HYDRODYNAMIC AND THE BFM BIOGEOCHEMICAL MODEL. THEY EXPLORE THE NUMERICAL EFFICIENCY OF THIS NEW COUPLED MODEL AND ASSESS THE TRADE-OFF BETWEEN COUPLING TIME STEPS AND SIMULATION SPEED. THE COUPLED MODEL IS SUCCESSFULLY TESTED IN AN IDEALISED AND A REALISTIC SETUP.
GENERAL COMMENTS
THE MANUSCRIPT'S SCIENTIFIC SIGNIFICANCE IS GOOD. ONE COULD STATE THAT THIS IS ONLY YET ANOTHER EXAMPLE OF A COUPLED SYSTEM BORNE OUT OF EXISTING SUBMODELS. MORE THAN JUST COMBINING THE TWO EXISTING SUBMODELS, HOWEVER, THE AUTHORS CREATE AN ADDED VALUE WITH THEIR DETAILED DESCRIPTION OF THE COUPLING PROCESS AND WITH THEIR CONCEPTUALLY MOD- ULAR APPROACH TO MODEL COUPLING THAT CAN BE (AND SHOULD BE) REUSED IN THE WIDER COM- MUNITY FOR SUBSEQUENT COUPLING ATTEMPTS.
THE SCIENTIFIC QUALITY OF THE MANUSCRIPT IS VERY GOOD. METHODS ARE EXPLAINED IN DE- TAIL, AND CONCLUSIONS ARE BASED SOLELY ON THE MATERIAL PRESENTED. I SHOULD BE FAIRLY STRAIGHTFORWARD TO REPRODUCE THE WORK INDEPENDENTLY; SOME INFORMATION ON UPGRADING THE GCHEM IS MISSING.
THE LANGUAGE USED IS CLEAR AND CONCISE; THE MANUSCRIPT IS WELL STRUCTURED, ALL TABLES AND FIGURES ARE HELPFUL. UNFORTUNATELY, THE TECHNICAL QUALITY OF THE FIGURES IS NOT REACHING THE STANDARD OF THE WRITTEN MATERIAL. ALL FIGURES SHOULD IMPROVED OR REDESIGNED. AT THE CURRENT STATE, THEY ARE NOT ACCEPTABLE FOR PUBLICATION. NEITHER IS THE MATHEMATICAL TYPESETTING WHICH ALSO NEEDS MAJOR IMPROVEMENTS.
We thank Dr. Lemmen for the positive comments and the important issues he raised. We improved the quality of the manuscript revising all the figures and the typesetting of the equations, variables and pieces of code. Furthermore, we carefully revised the abstract, the introduction, the model descriptions and the discussion according to the proposed suggestions.

SPECIFIC COMMENTS

ABSTRACT WITHIN THE ABSTRACT, THE MAIN PROPERTIES OF THE BFM SHOULD BE ADDED (E.G, THAT IT IS A NPZD TYPE MODEL). THE SENTENCE "EFFICIENT SCHEME THAT MANAGES COMMUNICATION AND MEMORY SHARING" NEEDS CLARIFICATION, AS IT IS NOT CLEAR WHAT "EFFICIENT" REFERS TO (MEMORY, TIME, ...). ALSO, TELL THE READER WHAT THE "EXPECTED THEORETICAL" AND THE "OBSERVED" BEHAVIOUR IS.
Thank you for the remarks: we revised the abstract as follows. We specified that BFM is a model based on plankton functional types formulation. We better introduced the characteristics of the new coupler, describing that is online, open source and that has been developed in a way that preserves the sustainability of the programming effort to handle future evolutions in the two codes.
Finally, we specified that our model reproduces the alternation of surface bloom and deep chlorophyll formation driven by the seasonal cycle of winter vertical mixing and summer stratification in the mid latitude gyre test case. Then we reported that the main features and spatial patterns of the hydrodynamic and biogeochemical variables in the Mediterranean domain are consistent with the literature.

P1 L33F THERE IS MUCH INFORMATION ON THE FEEDBACK OF BGC ON HYDRODYNAMICS, BUT THIS FEEDBACK IS NOT REALIZED IN THE MODEL PRESENTED. IT IS, HOWEVER USED TO MOTIVATE THE COUPLING OF HYDRODYNAMIC AND BGC MODELS. PLEASE DISENTANGLE.
We thank Dr. Lemmen for his thorough comments. Considering also other comments regarding the coupling issues (*P1L33, P2L6, P2L30 AND P3L10*), we have significantly modified the introduction, amending several parts. In particular, we have introduced a new paragraph (new text at P3L8-15) including the rationales for an online coupling of hydrodynamics and biogeochemistry, and we explained our motivations for choosing to couple MITgcm and BFM.
In doing that, we moved the sentences regarding the influences (and feedbacks) of physics on biogeochemistry to the new paragraph. In paricular, we explained that the motivations for online coupling are several (i.e., forcing the biogeochemistry at the same frequency as the hydrodynamic processes, avoiding the use of large files where to save hydrodynamic variables at high frequency, ensuring the use of consistent differential operators - advection and diffusion - for hydrodynamics and biogeochemistry) and the capability of describing possible feedbacks from biogeochemistry to hydrodynamics is just a potential that the online coupling could provide.

P2 L4 I DON'T AGREE WITH YOUR WORDING "BECAUSE OF". THE IMPROVEMENTS ARE NOT CAUSALLY RELATED TO BETTER COMPUTER RESOURCES; RATHER THESE INCREASED RESOURCES HAVE ENABLED THE INCLUSION OF MORE PROCESSES.

"Because of" has been removed, and the sentence has been revised. The concept we would like to communicate is that the development of models has become a cooperative and multidisciplinary task, rather than an individual effort, since the code complexity is increased because of the use of new programming paradigms (i.e., parallel programming) and the biogeochemical model has become more complex due to the inclusion of new variables and processes.

The sentences have been rewritten as follows: "In recent decades, the increasing availability of significant computational resources has allowed substantial improvements in hydrodynamic and biogeochemical models in terms of both temporal and spatial resolution of the simulations, which required new specific programming and coding expertise (i.e., code optimization and parallel programming). In addition, biogeochemical model complexity has increased through the inclusion of new variables and processes (Robson, 2014), and model development has become a cooperative and multidisciplinary task rather than an individual effort." at P2L13-17.

P2 L6 PLEASE PROVIDE A REFERENCE FOR INCREASED "FLEXIBILITY AND MODULARITY" OF APPLICATIONS. THIS IS NEITHER (AGAIN) CAUSED BY INCREASED RESOURCES, NOR DO I SEE MUCH EVIDENCE FOR INCREASED FLEXIBILITY AND MODULARITY YET. WHAT IS YOUR EXACT DEFINITION OF MODULARITY (AND FLEXIBILITY?)

Please consider the previous point: the concepts have been revised, the words removed and the sentences have been rewritten (See new sentences at P2L13-17).

P2 L15F I DISAGREE WITH THE STATEMENT "HYDRODYNAMIC CODES ARE FAR MORE COMPLEX THAN BGC CODES", AND I DISAGREE WITH THE WORD "BECAUSE". I THINK THE REASON IS HISTORIC, BECAUSE WE STARTED NUMERICAL SIMULATIONS WITH HYDRODYNAMIC MODELS AND ADDED MORE PROCESSES (AMONG THEM BGC) ONTO THE HYDRODYNAMIC MODEL. ONCE PHYSICAL OCEANOGRAPHERS CLAIMED THEIR STAKES IN HANDLING THESE HYDRODYNAMIC MODELS WITH BGC "APPENDICES" IT BECAME DIFFICULT FOR OTHER DISCIPLINES TO ESTABLISH AN ALTERNATE WORKING MODE, LIKE BUILDING A BGC MODEL WHERE THE HYDRODYNAMICS IS THE "SIMPLER" APPENDIX.

MOREOVER, THE SEEMINGLY COMPLICATED (NOT COMPLEX!) MATHEMATICAL DESCRIPTION AND NOTATION USED BY PHYSICAL OCEANOGRAPHERS (SEE EQS. 1–9 IN THIS MANUSCRIPT) MIGHT HAVE EXCLUDED RESEARCHERS FROM OTHER FIELDS TO DRIVE DEVELOPMENT OF COU- PLED HYDRODYNAMIC MODELS. AND WHILE THE MATHS INVOLVED IN SOLVING EQS. 1–9 IS CERTAINLY COMPLICATED, THE MANY MORE INTERACTIONS IN BIOLOGICAL SYSTEMS MAKE THE ECOLOGY AND BIOGEOCHEMISTRY THE MORE COMPLEX PART OF A COUPLED MODEL SYSTEM.

TALKING ABOUT CODE COMPLEXITY, MUCH OF THE CODE BASE OF PHYSICAL OCEAN MODELS IS CONCERNED WITH INPUT AND OUTPUT, WITH INFRASTRUCTURE TO DEFINE THE MODEL DOMAIN AND ITS BOUNDARIES, AND NOT THE HYDRODYNAMIC CORE. BGC CAN BE SLIMMER WHEN THEY ARE COUPLED TO SUCH OCEAN MODELS THAT PROVIDE ALL THE INFRASTRUCTURE. AND, OF COURSE, A MAJOR PROCESS (TRACER ADVECTION DIFFUSION) IS SHARED BY BOTH BGC QUANTITIES AND PHYSICAL QUANTITIES AND CONTRIBUTES TO CODE COMPLEXITY OF EITHER ONE (OR BOTH) THE BGC AND THE PHYSICAL MODEL.

We thank Dr. Lemmen for the clarification. Indeed, the sentence was written a bit "hastily"… We revised the sentence pointing out that the inclusion of the biogeochemical models into hydrodynamic ones (and not vice-versa) have occurred (to our knowledge) mainly because the hydrodynamic models had already been coded to solve the partial differential equation of tracers and had a coding infrastructure capable to handle the spatial-temporal properties of the simulations (i.e. bathymetry, boundaries, computational domain discretization).

The sentence has been revised as follows: " … because hydrodynamic codes have been already developed to solve the partial differential equation of tracers and provide the coding infrastructure to handle the spatial-temporal properties of the simulations (i.e. bathymetry, boundaries, computational domain discretization)" at P2L25-27.

P2 L16F "IS PREFERABLE" IS A VALUING STATEMENT THAT SHOULD BE AVOIDED. ALSO, THE REASON GIVEN "IT FACILITATES UPGRADES" IS NOT SUBSTANTIATED. IN CONTRAST, SOME MIGHT ARGUE THAT A CENTRALIZED/MONOLITHIC SYSTEM IS BETTER TO HANDLE W.R.T. UPGRADING. PLEASE ELABORATE (HERE OR AT A DIFFERENT SUITABLE PLACE)

We agree with the reviewer that we cannot argue which coupling philosophy is the best, because it depends on many factors (e.g., type of the models, size of scientific community working on them). Here we wanted to state that there can been different philosophies for coupling models: merging one model into the other, or develop a modular interface between the two. This part of the introduction has been rewritten at P2L22-29.

P2 L25FF NAME THOSE EXISTING COUPLINGS WITH MITGCM SPECIFICALLY, NAME THE "SPECIFIC HIGH-COMPLEXITY MODEL". WHY ARE THOSE COUPLED MODELS NOT "STATE-OF-THE-ART"; IF IT IS THE LACK OF MULTI-NUTRIENT/MULTI-SPECIES SUPPORT, THEN MAKE A CAUSAL STATEMENT.

"State-of-the-art" has been removed. The issue we would like to communicate is that there have already been experiences of coupling of the two models (MITgcm and BFM) with other models: they are suitable for being coupled, but they have never been coupled together. The sentences have been revised as follows: "The two models are widely used, as described in the next sections, and have been already coupled with several other models. For example, the MITgcm has already been coupled to low- (Parekh et al., 2005; Follows et al., 2006) or intermediate-complexity (Hauck et al., 2013, Cossarini et al., 2015a) biogeochemical models for a few specific applications and to a specific high-complexity model (Dutkiewicz et al., 2009) to explore the theoretical aspects of intraspecific competition in plankton communities. On the other side, the BFM has already been coupled to POM (Polimene et al., 2006), NEMO (Vichi and Masina, 2009; Epicocco et al., 2016) and to the offline OGSTM, an upgraded version of OPA (Lazzari, et al 2012). A direct coupling between MITgcm and BFM has not been implemented yet. Thus, we developed a dedicated online modular coupler linking them. The new coupler is open source and allows to exploit the high potentiality of the two models, to preserve the sustainability of the programming effort and to handle future evolution of the two codes" at P3L8-15.

P2 L30 YOU GIVE NO MOTIVATION WHY US DO NOT USE ONE OF THE EXISTING COUPLINGS OF BFM WITH ANOTHER HYDRODYNAMIC MODEL. PLEASE ELABORATE ON YOUR MOTIVATION TO DO YET ANOTHER COUPLING TO ANOTHER OCEAN MODEL. ALSO, I WOULD LIKE TO SEE A DISCUSSION WHY YOU DID NOT CONSIDER TO INCLUDE BFM IN THE FABM FRAMEWORK, AS THIS WOULD GIVE YOU INSTANT MODULAR COUPLING TO A MULTITUDE OF OCEAN MODELS THAT ALREADY IMPLEMENT FABM.

We revised this part of the introduction (please consider also our answer to point *P1L33F*). As regards the existence of FABM, we would like to inform the reader that alternative options for coupling hydrodynamic and biogeochemical models exist. Our choice for an online coupling based on a specifically developed coupler rises from both practical and historical reasons: in fact, we had good experiences in working with both MITgcm (e.g. Querin et al., 2013; Sannino et al., 2015) and BFM (e.g. Lazzari et al., 2012, 2016; Cossarini et al., 2015). Considering that, to our knowledge, FABM is neither coupled with MITgcm nor with BFM, and that quite some time is needed to acquire full competences for using a model, our object is to describe and provide the reader with a coupling scheme linking the two models, rather than testing different couplings of hydrodynamic and biogeochemical models. We acknowledge that it would be interesting to explore the potentials of FABM and to compare the efficiency of different couplers, however, this is beyond the scope of the present work.

P2 L33 "COUPLING TOOLS WERE NOT USED BECAUSE ... WANT TO PRESERVE PERFORMANCE". NOW THAT IS EXACTLY THE RAISON D'ETRE FOR A COUPLING TOOL LIKE ESMF, WHICH HAS BEEN PROVEN TO PRESERVE PERFORMANCE AND HAVE A VERY LOW OVERHEAD. A MORE IN-DEPTH DISCUSSION FOR NOT CHOOSING ESMF (OR SIMILAR) IS REQUIRED AT THIS POINT. AND, OF COURSE, A BETTER SUBSTANTIATION FOR YOUR CONCLUSION TO DISREGARD EXISTING COUPLING TOOLS.

We revised this part of the introduction (Please consider our response to point *P1L33F*).

P2 L38 HOW DO NUMERICAL ACCURACY AND GOOD PERFORMANCE LEAD TO FLEXIBILITY? I DONT' UNDERSTAND YOUR "THEREFORE". THROUGHOUT THE MANUSCRIPT, PLEASE MAKE SURE YOU ARGUE BOTH YOUR POINTS "PERFORMANCE" (WHICH IS WELL SUBSTANTIATED) AND "FLEXIBLITY" (LESS SO) CONSISTENTLY, OR DROP FLEXIBILITY AS A GOAL OF YOUR COUPLING IF NOT SUBSTANTIATED BETTER.

We used improperly the word "flexibility", and it has been removed. The intoduction has been substaintally revised (please, see comments to point *P1L33F*). Additionally, we have removed the word "Therefore". Here we would like to summarize that our results show that the coupled MITgcm-BFM model guarantees mass conservation of chemicals, has good computational performace and provides reliable results. Without making conjectures with regard to other couplers, we belive and show that our open source coupling package can be a promising tool for investigating marine biogeochemistry at different spatial and temporal scales.

*P3 L6 SOMETIMES, BGC MODELS DO *NOT* SOLVE EQUATIONS BUT PROVIDE TENDENCIES ONLY THAT ARE SOLVED BY THE HYDRODYNAMIC MODEL, AS WELL.*

Solve has been substituted with the more generic term "describe" at P3L29.

P3 L10 I WOULD AGREE TO IGNORE EFFECTS OF BGC ON HYDRODYNAMICS, BUT YOU USE EXACTLY THIS ARGUMENT TO MOTIVATE COUPLING IN YOUR INTRODUCTION. PLEASE RESOLVE THIS CON FLICT WITHIN YOUR MANUSCRIPT.
We substantially revised the part of the introduction dealing with this point. Please refer to our comments on the point *P1L33F*.

P3 L15FF THE TYPESETTING OF THE EQUATIONS IS POOR AND HINDERS UNDERSTANDING. IT IS UNACCEPTABLE FOR PUBLICATION, PLEASE USE PROFESSIONAL MATH TYPESETTING. MAJOR ISSUES ARE FONT SIZES AND SPACING WITHIN THE EQUATIONS, IT IS HARD TO SEE SUBSCRIPTS, IMPLIED MULTIPLICATIONS APPEAR IN SUBSCRIPT, BOLD FACE IS NOT CLEARLY DISTINGUISHABLE …
The typesetting of all equations has been complitely revised, using the appropriate Microsoft Equation objects (rather than the "Insert/Equation" tool).
We have introduced a new section 2.1 (Nomenclature and units) that explains the typesetting and convention used throughout the paper. Finally, as suggested, we added a new table (table B.1 in new appendix B) containing all the symbols and variables used throughout the text.

P3 L27 SUBSCRIPTS H AND V (HORIZONTAL, VERTICAL) NOT EXPLAINED
Done at P4L25. A new table (Appendix B) reports all symbols and variables used throughout the text.

P3 L28 ACRONYM RHS = RIGHT HAND SIDE NOT EXPLAINED
Done at P4L26.

P3 L29 THERE IS NOT PLAIN F, BUT SUBSCRIPTED F
Done, " $\mathbf{F}_H$ and F_V " added at P5L2.

*P4 L1 SEE ABOVE FOR TYPESETTING EQS. HERE, ESPECIALLY, THE PROBLEM WITH SUBSCRIPTS IS APPARENT. I SUGGEST THEY SHOULD BE UPRIGHT ROMAN IF WORDS (LIKE BIO, BFM) AND SPACE TO EXCLUDE MISUNDERSTANDING AS B * F * M IMPLICITLY.*
The equation has been revised, all tysetting corrected and BFM substituted with $\mathbf{R}_{\mathrm{bio}}$ according to the suggestion of reviewer#1.

P4 L8 "CAN BE HANDLED". WHO DECIDES TO HANDLE EQ. 8? THIS IS A SERIOUS MODULAR COUPLING ISSUE THAT DESERVES MORE DISCUSSION. WHAT IS YOUR SOLUTION, SPECIFICALLY AND WHY?
The coupling problem is described here in generic terms. The next section (2.4) of the manuscript will explain and discuss how the different terms are handled by the different pieces of code in our specific coupling. In order to communicate the generality of the topic, we have rephrased the sentence as follows "can be handled by either the hydrodynamic or the biogeochemical model, according to the specific processes and the features of the codes" at P5L20-21.

P4 L22 ALL CODE AND FILENAMES SHOULD BE IN A TYPEWRITER FONT. (I.E STARTING FROM "USE") AND ALSO "DATA.PKG"
Done. Further, we have introduced a new section 2.1 (Nomenclature and units) that explains the typesetting and convention used throughout the paper.

P4 L23 CHECK EXACT VERSIONING AND TYPESETTING FOR MODEL VERSION OF MITGCM
We used the MITgcm Release 1 – Checkpoint 65 k at P6L17

P4 L24 UNCLEAR TYPESETTING, WHY ALL CAPS TRACERS? PLEASE SET PTRACERS IN TYPE- WRITER FONT.
Done.

P5 L1FF TYPESETTING. YOU MAY CONSIDER TO INTRODUCE A SPECIFIC TYPESETTING SCHEME FOR YOUR CODE PARTS, BUT YOU NEED TO EXPLAIN IT BEFOREHAND. THIS APPLIES TO THE ENTIRE MANUSCRIPT.
Thank you for the suggestion. We have introduced a new section 2.1 that explains the convention and typesetting scheme applied to the entire manuscript.

P5 L1FF CONSIDER TO PUT THIS INFORMATION IN A TABLE.
Since it is a short list, we would prefer to leave the text as it is.

P6 L4 WHERE ARE THESE ALTERATIONS "UPGRADES" TO GCHEM DOCUMENTED? WHERE ARE THEY AVAILABLE (AS A PATCH?, IN THE MITGCM DISTRO?)
These alterations to `GCHEM` are explained in the `BFMCOUPLER` manual (appendix A) and the modified routines (`GCHEM_CALC_TENDENCY.F`, `GCHEM_READPARAMS.F`, `GCHEM_FIELDS_LOADS.F`, `GCHEM_INIT_FIXED.F` and `GCHEM_INIT_VARI.F`) are provided along with the `BFMCOUPLER` package in the GIThub repository. In particular, as explained in the manual, a `call` statement to a `BFMCOUPLER` routine must be added into the corresponding `GCHEM` routine.
In the main text we clarified this point by changing the sentence as follows "… by upgrading a few routines of the MITgcm package `GCHEM` (GeoCHEMistry, details in appendix A)," at P8L10-11.

P6 L36 THE STAR "" IS NOT A MATHEMATICAL SYMBOL*
Corrected. Thanks.

P6 L18 DO NOT EXTEND THE "≈" SIGN OVER THE SUBSCRIPT
Corrected. Thanks.

P8 L11,19 INCONSISTENT SUBSCRIPT "S" TO PAR AND MANY MORE EQUATION TYPESETTING PROBLEMS
Done. We carefully revised the typesetting of all the equations and symbols.

P9 L35 UNDER WHAT LICENSE IS BFMCOUPLER DISTRIBUTED (MIT)? ALSO NAME THE LICENSE FOR BFM (GPL) AT THE APPROPRIATE PLACE EARLIER IN THE TEXT. HOW DO THESE LICENSES PLAY TOGETHER. DID YOU INCLUDE ANY CODE PARTS FROM BFM INTO THE COUPLER AND HOW DID YOU DEAL WITH CHANGING THE LICENSE?
The BFM license is a GNU GPL license, and it has been added at P7L30.
Regarding the `BFMCOUPLER`, we decided for a GPL license in order to be consistent with the license of the BFM model. We believe that our package should be free to be copied, used, modified and published, being consistent with the philosophy of the BFM consortium (bfm-consortium.eu). A license note has been added to the `BFMCOUPLER` files in the GIThub repository. Thus, the final coupled code will work under the more restrictive license that, to our understanding, is the GPL.

P9 L35 WHO ENSURES LONG-TERM AVAILABILITY OF THE CODE IF HOSTED ON GITHUB? COULD THE CURRENTLY USED VERSION (WHICH GIT SHA?) BE ARCHIVED AND PROVIDED AS SOM?
A git SHA-1 hash string, linking the present release 1.0, has been added to the Code availability section in appendix A.
Regarding the long term availability of the code, we would like to point out that other codes published in Geoscientific Model Development are available through GIThub, and we believe that this service will continue ensuring the free availability of our code. However, the long term availability of the code will be also ensured by the modeling group of the OGS Institute (ECHO, http://www.inogs.it/en/content/echo-ecology-and-computational-hydrodynamics-oceanography). Indeed, a copy of the `BFMCOUPLER` project is now saved in other internal repositories and it is available upon request

P11 L40 DT_TRC IS NOT EXPLAINED, PLEASE CHECK ALL YOUR ACRONYMS AND SUBSCRIPTS FOR EXISTING EXPLANATIONS. CONSIDER A TABLE OF SYMBOLS.
The symbol has been corrected, and the sentence revised as follows: "With a LS_n set to 8 (a time step for tracers, Δt_{trc} , equals 2400 s), the" at P16L7. Further, we would like to remind that we have added a new table (Appendix B) reporting all symbols and variables in order to facilitate the reader.

P12 L6F PLEASE MOTIVATE YOUR CHOICE OF THE 0–200 M DEPTH RANGE FOR INTEGRATION OF CHL. MAYBE PROVIDE SOME INFOMATION ON THE TYPICAL DEPTH DISTRIBUTION OF CHL IN THIS REGION. ALSO, USE CORRECT TYPOGRAPHY (EN-DASH AND NOT HYPHEN BETWEEN NUMBER AND UNIT).
The depth of 200 m is the lowest limit of the photic layer in the Mediterranean Sea as reported in Lazzari et al. (2012). Thus, since the idealized case has been designed to reproduce condition similar to those of the Mediterranean Sea, we used this value to compute the integral of the chlorophyll values.

P12 L22 PROVIDE EVIDENCE THAT THE FLOATING POINT ROUNDING LED TO THIS ERROR. HOW IS THE MASS BUDGET AFFECTED BY DIFFERENT CHOICES OF THE LS OPTION?

We checked this aspect by performing several tests on the time-averaged files dumped by the model I/O routines (output dumped every month, 15 days, 5 days and 1 day) and on the precision of the output files (32 bit versus 64 bit).

The errors on the computation of mass conservation are due to the time discretization/average of the output files (rounding associated with the time average calculations of concentration and SSH). The errors are not due to the floating-point precision used to save the model output, as we erroneously wrote in the previous version of the paper. Therefore, we have redrawn Figure 7 using daily model output and we corrected the sentence as follows: "The errors in mass conservation over time were small ($O(10^{-9})$) and they were caused by the computation of the time average of the model output." at P16L29-30.

P13 L38 PCO2 NOT EXPLAINED, ALSO BAD TYPOGRAPHY.

pCO2 has been substituted with pCO_2^{atm} in Figure 1 and in the text. The term is explained when introduced at P18L23 and it is listed in the new table of appendix B.

P14 L5 FOR HOW MANY CORES DID YOU COME UP WITH A SIMULATION TIME OF 65 HRS PER YEAR?

Thank you for pointing this out. The number of cores was 224, decomposed in a grid of 16 x 14 cores. We have corrected the text.

P15 L29 I DON'T AGREE WITH THE TERM "FRAMEWORK". YOU DESCRIBE A COUPLING AND A COUPLING STRATEGY, BUT CERTAINLY NOT A FRAMEWORK.

The word "framework" has been removed.

P16 L3FF THIS PARAGRAPH IS ENTIRELY UNCLEAR TO ME. BOTH FABM AND MESSY ARE CAPA- BLE OF DOMAIN DECOMPOSITION AND HAVE BEEN SHOWN TO SCALE VERY WELL. PLEASE BETTER SUBSTANTIATE OR ARGUE YOUR REASONS NOT TO USE THESE SOMEHOW ESTABLISHED COUPLING FRAMEWORKS.

We agree: this paragraph was not clear. We simply meant that the efficiency of a coupled code can be an issue. Our coupling (as others like FABM and MESSy) is capable to handle this aspect.

The sentence has been rewritten as follows: "Despite the growth of computational resources, the efficiency of coupled codes can be still an issue because of the large size of the computational grids (Blom and Verwer, 2000). Domain decomposition and parallelization tools are available in several coupling environments (e.g., FABM, Bruggeman and Bolding, 2014; and MESSy, Jöckel et al., 2008). Likewise, our coupling scheme has been thought to fully exploit the parallelization efficiency of the MITgcm (Marshall et al., 1997), and no additional coding effort (in terms of parallelization) is required by the users." at P21L13-17.

P17 L10 I WOULD RECOMMEND TO ADD A SECTION AND PARAGRAPH "CODE AVAILABILITY" HERE WITH THE WEB RESOURCES, GIT/ARCHIVE INFORMATION, VERSION NUMBERS, AND LICENSES. MOVE THE CONTENT FROM APPENDIX A4 HERE TO THIS MAIN SECTION.

Thank you for the suggestion, however, we would rather leave the section A4 in the appendix. The manual (appendix A) and the availability of the code are already mentioned in the main text; and we think that appendix A should end with the indication of the code availability and the description of the experiment that can be downloaded.

However, we will agree to move section A4 into the main text if the reviewer or the editor still recommends doing so.

FIGURE 1 SPELLING OF OMNIVOROUS, OXIDATION. FROM THE FIGURE, IT IS UNCLEAR WHAT THE SUPERSCRIPT NUMBERS (1) ETC. DENOTE, PLEASE EXPLAIN. IF (AS I BELIEVE) THIS IS A MERE INDEX, THEN THE NOTATION IS RATHER UNUSUAL AND CONFUSING. COULD YOU FIND A BETTER NOTATION OR MAKE TRANSPARENT WHY YOU USE THIS ONE? WHY DO YOU NOT USE THE SUBSCRIPT I FOR YOUR INORGANIC NUTRIENTS BUT SPELL THEM OUT, THIS IS INCONSISTENT.

Thank you for the comment. We made the following changes to the new version of the figure: correction of omnivorous, oxidation; revision of the typesetting of the BFM variables (Helvetica) and subscript for

chemical element (blackboard style), revision of all lines and boxes in order to improve the graphical aspect.
Then, the superscript numbers (e.g. (1)) are mere index used to compose the variable's name in the BFM nomenclature (e.g. $N_P^{(1)}$ equals to `N1p` in the BFM code). This convention is explained in the BFM manual and references thereby. Therefore, in preparing Figure 1, we would prefer to maintain the convention adopted by the BFM consortium since, even if it is not the best notation, it would help the reader to get acquitted with the BFM convention.
Further, the caption has been upgraded as follows: "Figure 1: BFM model: scheme of the functional interactions among the variables in the version that was implemented in Lazzari et al. (2012), Melaku Canu et al. (2015), and Cossarini et al. (2015b). Variable names follow the BFM convention (Vichi et al., 2015). The subscripts indicate the chemical components ($\mathbb{C}$: carbon; $\mathbb{P}$**:** phosphorus, $\mathbb{N}$**:** nitrogen, $\mathbb{S}$**:** silica, $\mathbb{O}$**:** oxygen)**.**"

FIGURE 2 THERE IS A NEED TO SYNCHRONIZE ALL SYMBOLS WITH THOSE USED IN THE MAIN TEXT, ALSO REFER TO THE (SUGGESTED) TABLE OF SYMBOLS, IF AVAILABLE. SOME SIMPLIFICATIONS IN TERMINOLOGY COULD HELP, WHY E-P-R, IF EPR IS SUFFICIENT—OR CALL IT MOISTURE BALANCE; WHY THE SUM OF QX WHERE QΘ IS SUFFICIENT. HELP THE READER DISTINGUISH BETWEEN C FOR CARBON AND C FOR CONCENTRATION, ESPECIALLY AS SUBSCRIPT; MAKE SURE THE NOTATION ALIGNS WITH FIGURE 1.
The style of the figure has been revised according to the reviewer's suggestions. In the new version of Figure 2, the symbols have been synchronized with those used in the main text, and the typesetting has been resived as well (variables in italic, code and package names in Courier font, name of models and other text in Helvetica font). The sum of heat fluxes has been substituted with the Q; E-P-R has been substituted with *EmPmR* which is the convention used by MITgcm.
A new section 2.1 explains the convention used throughout the text, and a new appendix (Appendix B) reports all the symbols used in the manuscript.

*FIGURE 3 ALIGN TYPESETTING WITH (REVISED) TYPESETTING IN-TEXT. CLEAN UP, E.G., WHY PTRACER AND PTRACER IN THE SAME FIGURE? PLEASE EXPLAIN, HOW YOU NUMERICALLY HANDLE THE EQUATION PTRACER=PTRADERS + DT*GCHEMTENDENCY WITH REGARD TO CFL AND POSSIBLE UNDER/OVERFLOWS.*
Figure 3 has been revised according to the reviewer's suggestions. In particular, normal text is in Times New Roman, code and routine names are in typewriter style, variables in italic.
All variables (e.g., *pTracer*) have been carefully revised and corrected.
Finally, the numerical integration of the derivative for *pTracer* is handled by the `TIMESTEP_TRACER` MITgcm routine (Euler forward scheme). The CFL condition is intrinsically satisfied in `GAD_CALC_RHS` and in the other routine that calculate the advection and diffusion terms (`GAD_ADVECTION`, or other routine according to the selected option).

FIGURE 4 THANKS FOR CHOOSING AN ACCESSIBLE COLORMAP! AVOID REDUNDANCY IN GRAPH (OF GEOGRAPHIC LOCATION), DO NOT LET AXIS LABELS OVERLAP. PROVIDE MORE CONTEXT IN THE CAPTION TO WHICH EXPERIMENT (I.E. IDEALIZED CLOSED BASIN) THIS GRAPH BELONGS. MOVE UNIT FROM CAPTION TO COLORBAR; CLARIFY WHETHER THIS IS MAGNITUDE OF 3D SPEED OR MAGNITUDE OF SPEED PROJECTED ON Z-PLANE.
The figure and the caption have been modified according to reviewer's suggestions.

FIGURE 5 REMOVE NEGATIVE SIGNS WHEREVER POSSIBLE. DEPTH IS USUALLY A POSITIVE NUMBER INCREASING FROM THE SURFACE DO THE BOTTOM, ADHERE TO THIS MORE COMMON CONVEN- TION. DO NOT DENOTE THE CONTOUR WITH A MINUS SIGN: CONCENTRATIONS AND NPP CANNOT BE NEGATIVE (THAT'S THE FIRST IMPRESSION I GET...). GIVE COLOR-CODED AND CONTOURED QUANTITY AT THE SAME PLACE IN THE FIGURE, LIKE "COLOR: T, CONTOUR: MLD". MAKE SURE YOU EXPLAIN ALL ACRONYMS, SOMETIMES A WORD MIGHT WORK INSTEAD OF THE SYMBOL, E.G. "TEMPERATURE" INSTEAD OF T. BE CONSISTENT WITH UNITS AND EXPONENTS. MOVE UNIT OF COLOR-CODED QUANTITY TO COLORBAR. ROTATE THE "M" UNIT ON Y-AXIS AS IT FALSELY GIVES THE IMPRESSION OF AN "E" AT FIRST GLANCE; ADD "DEPTH" TO Y-AXIS TO HELP THE READER. AVOID OVERLAP OF NUMBERS BETWEEN GRAPHS. SPELL HOVMÖLLER WITH A "V". GIVE CONTEXT ON EXPERIMENT AS IN FIGURE 4. MAKE SURE FONT SIZES ARE SIMILAR TO FIGURE 4, 6 (AND ALL OTHER FIGURES).
The figure has been redrawn considering all the suggested points. Further, the caption has been rewritten as follows: "Figure 5: Hovmöller diagrams of the (a) Temperature and evolution of the mixed layer depth (MLD), (b) Phosphate and PAR, (c) Chlorophyll (sum of the chlorophyll content in the four phytoplankton functional groups) and Phytoplankton expressed in carbon biomass, (d) Oxygen and Net

Primary Production (NPP), (e) Small Zooplankton (Small Zoopl) and Mesozooplankton (Mesozoopl), and (f) bacteria."

FIGURE 6 AGAIN, USE CONSISTENT EXPONENTS, EXPLAIN ALL ACRONYMS. ADD MORE MEANING TO THE VERY TECHNICAL CAPTION. PAY ATTENTION TO DETAIL LIKE THE MISMATCH BETWEEN THE STATEMENT "ROOT MEAN SQUARE ERROR" AND RMSD (UNEXPLAINED, BUT I SUPPOSE "DEVIATION"); ADD YOUR CHOICE OF ACCEPTABLE RMSD THRESHOLD TO GRAPH. CONSIDER USING STACKED BARS INSTEAD OF AREA PLOT FOR LEFT AXIS. IMPROVE LOOKS OF FIGURE.

Figure 6 has been redrawn using stacked bars instead of areas for left axis. Names in the legend are better explained in the caption, as well as RMSD, which is now consistent with the text in the caption. The caption has been rewritten in order to clarify the different terms that appear in the legend.

FIGURE 7 EXPLAIN "ETA" (OR USE GREEK SYMBOL AS SUGGESTED FOR TEXT, AND ADD SEMANTICS FOR SEA SURFACE HEIGHT), TAUTOLOGY "ALKALINITY CONCENTRATION", USE CONSISTENT NAME "ALKALINITY" OR "TOTAL ALKALINITY". ALIGN STYLE OF FIGURE TO OTHER FIGURES IN YOUR MANUSCRIPT. REPLACE "1 LAYER" WITH "SURFACE LAYER". IMPROVE OVERALL LOOK OF FIGURE (TICKS, LEGEND, LINE WIDTH/STYLES, LABELS, TITLE ,....).

The figure has been redrawn using daily model output instead of 15-day averages (see comment P12L22) and the general layout has been improved. In particular, Eta has been substituted with Sea Surface Height (SSH), alkalinity label has been corrected, units are consistent with the main text, font size has been increased, and ticks have been aligned.

The caption has been rewritten as follows: Figure 7: Evolution of SSH (blue line) and alkalinity (red line) at the surface layer together with the relative variation of total alkalinity mass (M) with respect to the initial condition (M0) over the whole domain (black line). The total alkalinity mass was obtained by multiplying the daily average model output by the domain volume, which included the time-varying SSH at the surface layer.

FIGURE 8 IMPROVE OVERALL FIGURE QUALITY. CHOOSE MORE CONTRAST FOR DEPTH COLORMAP (CONSIDER ESTABLISHED TERRAIN/OCEAN FLOOR COLORMAPS); LARGER FONT SIZES THROUGHOUT. UNIT OF GEOGRAPHIC COORDINATES IS DEGREE N OR E. ADD PADDING BETWEEN TEXT AND FIGURE MARGINS. MAKE ALL NAMED FEATURES (RIVER ENTRY POINTS, SITE LOCATION, OTRANTO STRAIT) MORE VISIBLE. POSSIBLY COMBINE WITH FIGURE 9 SHOWING 3 PANELS ALONGSIDE? THE LINE SHOWING OTRANTO STRAIT IS NOT IDENTICAL TO THE EXTENT SHOWN IN FIGURE 11.

Figure 8 has been completely redrawn. The quality of the figure has been improved. Longitude and latitude labels have been corrected and are now consistent with those of Figure 9. All named features have been made more visible. And the extent of line showing the Otranto Strait has been corrected.

Two new dashed lines have been added to show the two open boundaries: the Sicily Channel and the Cretan Passage.

FIGURE 9 AVOID REDUNDANCY IN Y-AXIS (LATITUDE); BE CONSISTENT WITH UNIT (SEE FIGURE 8), IT IS NOT HELPFUL TO SHOW 10 TIMES "N" ALONG THE AXIS. S NOT EXPLAINED, AGAIN DIFFERENT NOTATION FOR CHLOROPHYLL (CHLA, IN OTHER PLACES CHL). ADD INFORMATION ON COUNTROU QUANTITY IN THE PLOT (NEAR THE COLORBAR). PANEL A) SURFACE CURRENT MAGNITUDE NEEDS A SCALE BAR. PANEL B) I PREFER CHL TO BE SHOWN ON A LOG SCALE. BLUE CONTOUR UNFORTUNATELY COLLIDES WITH BLUE COLOR IN IONIAN BASIN, TRY DIFFERENT COLOR FOR THIS CONTOUR.

Figure 9 has been redrawn improving its quality. In particular in plot (b) a logarithmic color scale has been adopted for chlorophyll. This helped to make the blue contour (NPP) more distinguishable from the color plot. Variables are now clearly listed in the plot and their names are consistent with those used in the text.

Further, the caption has been changed accordingly.

FIGURE 10 NEGATIVE DEPTH AXES, LOG SCALE, COLLIDING LINES AND TEXT, FONT SIZES, MISLEADING Y-AXIS LABEL... PLEASE PAY ATTENTION TO THESE DETAILS. SUGGESTION: ADD "ADRIATIC PIT" AND "IONIAN DEEP" TO A) AND B) TO IMPROVE INTUITIVE ACCESS TO FIGURE. VISUALLY SEPARATE YEARS AND SPELL OUT THE FULL YEAR 2008 ETC. UNDER THE X-AXIS. ADD "CONTOUR" IN CAPTION

Figure 10 has been changed as follows: convention of depth axes is now consistent with the reviewer suggestion, font sizes have been revised, years have been spelled out and ticks to x-axes added, the labels "Adriatic Pit" and "Ionian Sea" have been added to (a) and (b) respectively.

Then, we tested logarithmic colorscale for chlorophyll, however, the graphical results were not satisfying, therefore we decided to keep the current colorscale.

The caption has been revised as follows: “Hovmöller diagrams of chlorophyll (color) and phosphate (contour, [mmol m^{-3}]) and plots of the mixed layer depth (dashed lines, [m]) for the southern Adriatic Pit (a) and the Ionian offshore area (b).”

FIGURE 11 NEGATIVE DEPTH AXES, COLLIDING LINES AND TEXT AND COLLIDING TEXTS, MISSING AXIS LABELS, UNDEFINED ACRONYMS ... AVOID REDUNDANT X-AXIS (LONGITUDE) INFORMATION, ADD UNITS TO COLORBAR, ADD CONTOUR INFO WITHIN FIGURE. CONSIDER DIFFERENT SCALING OF COLORED QUANTITIES, E.G. LOG OR SQUARE ROOT (WITH WORKAROUND FOR NEGATIVE VALUES) TO SHOW MORE DETAIL IN THE SMALL NUMBERS. ADDED SEMANTICS LIKE “VERTICAL SECTION” TO CAPTION.

Several changes have been made to Figure 11. In particular, a new colorscale has been adopted. The contour lines of the velocity field are blue and red for southward and northward velocities, respectively. The x-axis of the upper panel has been removed. Legends and texts have been made bigger and more readable.

The caption has been improved as follows: “Fluxes of organic carbon (upper panel) and DIC (lower panel) across the Otranto Strait (dashed line in Fig. 8). The solid contours specify northward (red) and southward (blue) meridional velocities.”.

TECHNICAL CORRECTIONS

P2 L7 “IS” SHOULD BE “HAS BECOME”

Done.

P2 L40 “FOLLOWING” SHOULD BE “SUBSEQUENT”

Done.

P3 L8 DELETE “VERY”

Done.

P4 L22 COMPOSED OF

Done.

P4 L31F USE A PROPER EM-DASH AND NOT A HYPHEN

Done.

P5 L11 “CUSTOM” INSTEAD OF “CUSTOMARY”

Done.

P11 L25 WELL-LIT, NOT “WELL-LIGHTED”

Done.

P12 L17 “ETA” SHOULD H?

Eta has been substituted with SSH here and throughout the manuscript.

P13 L35FF USE CONSISTENT EXPONENT, E.G, EITHER M−1 OR 1 OR 1/M, BUT ONLY USE ONE OF THOSE STYLES IN THE TEXT. I PREFER THE FIRST WITH NEGATIVE EXPONENT. CHECK ENTIRE MANUSCRIPT.

The entire manuscript has been checked for consistent exponents (e.g. m^{-1} convention is used)

P15 L1 “CONSISTENT” NOT “CONSISTENTLY”

Done.

Reference used in the present letter:

Cossarini, G., Lazzari, P. and Solidoro, C.: Spatiotemporal variability of alkalinity in the Mediterranean Sea. Biogeosciences, 12(6), 1647-1658, 2015.

Melaku Canu D., Ghermandi, A., Nunes, P.A., Lazzari, P., Cossarini, G. and Solidoro, C.: Estimating the value of carbon sequestration ecosystem services in the Mediterranean Sea: An ecological economics approach. Global Environmental Change. 32, 87-95, 2015.

Lazzari, P., Solidoro, C., Ibello, V., Salon, S., Teruzzi, A., Béranger, K., Colella, S. and Crise, A: Seasonal and inter-annual variability of plankton chlorophyll and primary production in the Mediterranean Sea: a modelling approach.Biogeosciences, 9, 217-233, doi:10.5194/bg-9-217-2012, 2012.
Lazzari, P., Solidoro, C., Salon, S. and Bolzon, G.: Spatial variability of phosphate and nitrate in the Mediterranean Sea: A modeling approach. Deep Sea Research Part I: Oceanographic Research Papers, 108, 39-52, 2016.
Sannino, G., Carillo, A., Pisacane, G., Naranjo, C., 2015. On the relevance of tidal forcing in modelling the Mediterranean thermohaline circulation Prog. Oceanogr. 134, pp. 304-329 doi:10.1016/j.pocean.2015.03.002
Teruzzi, A., Dobricic, S., Solidoro, C. and Cossarini, G.: A 3D variational assimilation scheme in coupled transport-biogeochemical models: Forecast of Mediterranean biogeochemical properties, Journal of Geophysical Research: Oceans, 119(1), 200-217, 2013.

Development of BFMCOUPLER (v1.0), the coupling scheme that links the MITgcm and BFM models for ocean biogeochemistry simulations

Gianpiero Cossarini[1], Stefano Querin[1], Cosimo Solidoro[1], Gianmaria Sannino[2], Paolo Lazzari[1], Valeria Di Biagio[1], Giorgio Bolzon[1]

[1]Department of Oceanography, Istituto Nazionale di Oceanografia e di Geofisica Sperimentale - OGS, Sgonico (TS), 34010, Italy
[2]UTMEA-CLIM Laboratory, ENEA, Rome, 00123 Italy

Correspondence to: Gianpiero Cossarini (gcossarini@inogs.it)

Abstract. In this paper, we present a coupling scheme between the Massachusetts Institute of Technology general circulation model (MITgcm) and the Biogeochemical Flux Model (BFM). The MITgcm and BFM are widely used models for geophysical fluid dynamics and for ocean biogeochemistry, respectively, and they benefit from the support of active developers and user communities. The MITgcm is a state-of-the-art general circulation model for simulating the ocean and the atmosphere. This model is fully three dimensional (including the non-hydrostatic term of momentum equations) and it is characterized by a finite-volume discretization and a number of additional features enabling simulations from global ($O(10^7)$ m) to local scales ($O(100)$ m). The BFM is a biogeochemical model based on plankton functional types formulations, and it simulates the cycling of a number of constituents and nutrients within marine ecosystems. The online coupling presented in this paper is based on an open source code, and it is characterized by a modular structure. Modularity preserves the potentials of the two models, allowing for a sustainable programming effort to handle future evolutions in the two codes. We also tested specific model options and integration schemes to balance the numerical accuracy against the computational performance. The coupling scheme allows us to solve several processes that are not considered by each of the models alone, including light attenuation parameterizations along the water column, phytoplankton and detritus sinking, external inputs, and surface and bottom fluxes. Moreover, this new coupled hydrodynamic-biogeochemical model has been configured and tested against an idealized problem (a cyclonic gyre in a mid-latitude closed basin) and a realistic case study (central part of the Mediterranean Sea in 2006-2012). The numerical results consistently reproduce the interplay of hydrodynamics and biogeochemistry in both the idealized case and Mediterranean Sea experiments. The former reproduces correctly the alternation of surface bloom and deep chlorophyll maximum dynamics driven by the seasonal cycle of winter vertical mixing and summer stratification; the latter simulates the main basin-wide and mesoscale spatial features of the physical and biochemical variables in the Mediterranean, thus demonstrating the applicability of the new coupled model to a wide range of ocean biogeochemistry problems.

1 Introduction

Coupling different models that have been specifically developed to study only limited aspects of the Earth's systems is becoming increasingly common due to the need to simulate different environmental components – and their interactions – simultaneously (Heavens et al., 2013). As regards numerical oceanography, coupled hydrodynamic-biogeochemical models are widely used to investigate and predict the physical, biogeochemical and ecological properties of marine ecosystems across a wide range of scales and provide useful tools that support environmental management and policies.

The numerical implementation of a coupling framework between three-dimensional hydrodynamic models and biogeochemical models is not a trivial task (Bruggeman and Bolding, 2014) because every model focuses on processes that occur on different temporal and spatial scales and uses different numerical parameterizations and schemes. Additionally, these models might be coded in different languages or follow different coding 'philosophies' with respect to memory allocation, computational schemes and code workflow. Furthermore, hydrodynamic and biogeochemical models are often developed by different and highly specialized scientific groups, whereas coupling requires interdisciplinary expertise.

In recent decades, the increasing availability of significant computational resources has allowed substantial improvements in hydrodynamic and biogeochemical models in terms of both temporal and spatial resolution of the simulations, which required new specific programming and coding expertise (i.e., code optimization and parallel programming). In addition, biogeochemical model complexity has increased through the inclusion of new variables and processes (Robson, 2014), and model development has become a cooperative and multidisciplinary task rather than an individual effort. A large number of generic, open-source models are utilized by the scientific community, and they can be customized to match the users' specific applications. A non-exhaustive list of the main state-of-the-art, hydrodynamic community models includes the MITgcm (Adcroft et al., 2016), GOTM (Burchard et al., 2006), ROMS (Haidvogel et al., 2000) and NEMO (Madec, 2014), whereas examples of community biogeochemical models include the BFM (Vichi et al., 2015), ERSEM (Butenschön et al., 2016), PISCES (Aumont et al., 2015) and ERGOM (Neumann, 2000).

Hydrodynamic and biogeochemical models can be coupled by merging their codes into a single larger new code, in which the original parts are intertwined. In this case, biological models are inserted into the workflow of the existing hydrodynamic model code (Burchard et al., 2006, Follows et al., 2006) because, in general, hydrodynamic models have been already developed to solve the partial differential equation of tracers and provide the coding infrastructure to handle the spatial-temporal properties of the simulations (i.e., bathymetry, boundaries, computational domain discretization). Alternatively, a modular approach can be adopted: each component preserves its own peculiarities, the coupling is performed only on localized portions of the code, and there are clear application programming interfaces (APIs). The separation of the two coupled components facilitates the maintenance of each code within its development community, avoids possible large efforts in solving the language differences between models and eliminates the need to keep models up to date with respect to the parent model. As an example, Bruggeman and Bolding (2014) proposed a set of programming interfaces (FABM) that allows communication between different hydrodynamic and biogeochemical models.

In this paper, we present a coupling scheme between the MITgcm hydrodynamic model and the BFM biogeochemical model for ocean biogeochemical simulations. The two models are widely used, as described in the next sections, and have been already coupled with several other models. For example, the MITgcm has already been coupled to low- (Parekh et al., 2005; Follows et al., 2006) or intermediate-complexity (Hauck et al., 2013, Cossarini et al., 2015a) biogeochemical models for a few specific applications and to a specific high-complexity model (Dutkiewicz et al., 2009) to explore the theoretical aspects of intraspecific competition in plankton communities. On the other side, the BFM has already been coupled to POM (Polimene et al., 2006), NEMO (Vichi and Masina, 2009; Epicoco et al., 2016) and to the offline OGSTM, an upgraded version of OPA (Lazzari, et al 2012). A direct coupling between MITgcm and BFM has not been implemented yet. Thus, we developed a dedicated online modular coupler linking them. The new coupler is open source, and allows to exploit the high potentiality of the two models, to preserve the sustainability of the programming effort and to handle the future evolution of the two codes. Further, the online coupling of hydrodynamic and biogeochemical models allows to drive the biogeochemistry at the same frequency of the hydrodynamic processes, avoiding the use of large files where to save hydrodynamic variables at high frequency. It also ensures the use of consistent differential operators (advection and diffusion) for hydrodynamic and biogeochemical variables, and would eventually provide a framework to describe possible feedbacks from biogeochemistry to hydrodynamics.

We demonstrate that the new online coupled model provides reliable results when simulating different marine ecosystems by correctly reproducing the interplay between physical, chemical and biological processes and components. The coupled model also runs with good computational performance and preserves the numerical accuracy of the solution. We consider that the MITgcm-BFM model represents a promising tool for investigating marine biogeochemistry at different spatial and temporal scales.

This paper is organized as follows. After a brief presentation of the two models (section 2), we focus on the technical aspects of the coupling algorithm. In the subsequent section (section 3), we describe the testing of the new coupled hydrodynamic-biogeochemical model against the idealized case of a cyclonic circulation in a closed basin and against a real case study in the central Mediterranean Sea. The paper closes with a discussion of the key issues of the coupling and future perspectives. A manual of the new code package is detailed in the Appendix.

2 Formulation of the hydrodynamic-biogeochemical coupling

A coupled hydrodynamic-biogeochemical model is composed of three main elements: a hydrodynamic sub-model, which solves the governing equations for oceanic flows; a tracer transport sub-model, which solves for the transport (advection and diffusion) of biogeochemical variables (commonly called tracers); and a biogeochemical sub-model, which describes the relationships (i.e., biogeochemical reactions) among the biogeochemical variables.

Following the common practice in which the biological feedback on transport is negligible, one can assume that changes in biogeochemical properties do not affect the water velocity, density or other physical properties; therefore, modifying the standard equations that underpin hydrodynamic models is unnecessary. We adopted such an assumption for this numerical coupling framework; however, this coupler was developed, in principle, to also handle biological feedbacks on hydrodynamics. The coupled model solves the set of partial differential equations specified below:

$$\frac{d\mathbf{v}_H}{dt} + f\mathbf{k} \times \mathbf{v}_H + \frac{1}{\rho_c}\nabla_H p' = \mathbf{F}_H \quad (1)$$

$$\varepsilon_{nh}\frac{dw}{dt} + \frac{g\rho'}{\rho_c} + \frac{1}{\rho_c}\frac{\partial p'}{\partial z} = \varepsilon_{nh} F_V \quad (2)$$

$$\nabla_H \cdot \mathbf{v}_H + \frac{\partial w}{\partial z} = 0 \quad (3)$$

$$\rho' = \rho(\theta, S, p(z)) - \rho_c \quad (4)$$

$$\frac{d\theta}{dt} = Q_\theta \quad (5)$$

$$\frac{dS}{dt} = Q_S \quad (6)$$

$$\frac{d\mathbf{C}}{dt} = \mathbf{Q_C} + \mathbf{R}_{bio} \quad (7)$$

$$PAR = PAR(Q_{sw}, \mathbf{C}) \quad (8)$$

$$\frac{d}{dt} = \frac{\partial}{\partial t} + \mathbf{v}_H \cdot \nabla \quad (9)$$

Momentum conservation equations, Eq. (1-2), continuity and density equations, Eq. (3-4), and active-tracers equations (for potential temperature θ and salinity S), Eq. (5-6), are formulated according to the semi-compressible Boussinesq approximation. In the equations, $\mathbf{v}_H = (u, v)$ is the horizontal component of velocity, w is the vertical velocity, f is the Coriolis parameter, ρ_c is a constant reference density, and p' is the pressure term. The right hand side (RHS) terms in Eq.

(1-2) and Eq. (5-6) correspond to the forcing and dissipation terms, including the diffusion, which acts on the momentum ($\mathbf{F}_H$ and F_V in Eq. (1-2)) and on the temperature and salinity (Q_θ and Q_S in Eq. 5-6). Similarly, Equation (7), which stands for a system of partial differential equations of tracers (**C**), encompasses the forcing and dissipation terms for biogeochemical tracers, $\mathbf{Q}_C$, and the biogeochemical reactions that occur in the sea, $\mathbf{R}_{bio}$.

Eq. (8) is an equation of state that calculates the modulation of irradiance *PAR* (photosynthetic active radiation) with depth starting from short-wave surface radiation fields (Q_{sw}). The total derivative accounts for the partial derivative in time and the advection term, which is related to the flow field, Eq. (9).

By adopting a more explicit formulation and commonly used assumptions based on scale analysis (see Crise et al., 1999), Eq. (7) can be rewritten as follows:

$$\frac{\partial \mathbf{C}}{\partial t} = -\mathbf{v}\cdot\nabla(\mathbf{C}) + \nabla_H(K_H\nabla_H(\mathbf{C})) + \frac{\partial}{\partial z}\left(K_V\frac{\partial \mathbf{C}}{\partial z}\right) + w_{bio}\frac{\partial \mathbf{C}}{\partial z} + \mathbf{R}_{bio}(\theta, S, \rho, PAR, \mathbf{C}) \qquad (10)$$

The first three terms on the RHS of Eq. (10) represent the advection (first term) and diffusion (second -horizontal- and third -vertical- term) of biogeochemical tracers, where K_H and K_V are the horizontal and vertical diffusivities, respectively, which are considered separately because they have different spatial scales. The remaining terms describe the sinking processes that affect biological particles (fourth term) and biogeochemical reactions (fifth term).

Within a coupled model, Eq. (1-6) are solved by the hydrodynamic sub-model, whereas Eq. (10) is solved partly by the transport sub-model, which is usually embedded into the hydrodynamic code, and partly by the biogeochemical sub-model. The other components, such as Eq. (8), the biogeochemical tracers forcing terms ($\mathbf{Q}_C$, e.g. surface and bottom boundary conditions) and the sinking terms, can be handled by either the hydrodynamic or the biogeochemical model, according to the specific processes and the features of the codes.

A coupler is defined as the interface that transfers the hydrodynamic information from Eq. (1-6) to Eq. (10) and controls the communication between the different terms of Eq. (10). In this study, the sub-models coupled are the MITgcm (managing both hydrodynamics and transport) and BFM (for the biogeochemistry) models, which are described in Sect. 2.2 and 2.3. The algorithm used to construct the fully coupled system is detailed in Sect. 2.4.

2.1 Nomenclature and units

Throughout the text, we used the following convention. In equations and text, *C* refers to the concentration (mass per unit volume) of biogeochemical model state variables, which are referred to as *pTracer* (passive tracer) in the MITgcm nomenclature. As regards BFM, the chemical components in the subscript are in blackboard style ($\mathbb{C}$: carbon; $\mathbb{N}$: nitrogen; $\mathbb{P}$:

phosphorus; S: silica). The pieces of code and the name of the routines and files are in typewriter font. Appendix B reports a list of all symbols and variables used throughout the text.

2.2 MITgcm

The MITgcm (Massachusetts Institute of Technology general circulation model; Marshall et al., 1997) is a three-dimensional, finite-volume, general circulation model used by a broad community of researchers. It can be customized to create different simulation set-ups by modifying its packages and parameters accordingly (Adcroft et al., 2016) and it has already been successfully applied to a wide range of case studies for the world's ocean at various spatial and temporal scales. The code and documentation of the MITgcm are under continuous development. The modular Fortran77 code is open source (Copyright (c) 2016 MITgcm Developers and Contributors), and it can be downloaded from the MITgcm website (http://mitgcm.org/) as a TAR file or using a CVS pserver. The most recent online documentation can be found at http://mitgcm.org/public/r2_manual/latest/. The MITgcm, which is designed to run on high performance computing (HPC) platforms, can solve fully non-hydrostatic and hydrostatic equations and can handle different free surface formulations. Subgrid-scale turbulence in both the horizontal and vertical directions can be parameterized by using different types of closure schemes with either constant or variable coefficients (e.g., Gent-McWilliams, Redi, Leith, Smagorinsky, KPP and GGL90). MITgcm code is composed of several packages, and depending on the selected experiment, the compiled packages can be enabled or disabled during the runtime by specifying the flag `use`*`PACKAGENAME`*`=.TRUE./.FALSE.` in the `data.pkg` input namelist. The MITgcm's implementation in this paper was based on the Release 1 - Checkpoint 65 k (April 2015) version of the code. Among the different available customization options, we adopted the fully implicit barotropic time stepping for the free surface, which is unconditionally stable. The vertical diffusion and viscosity terms in the horizontal momentum equations were treated implicitly in time and were solved by using the Euler backward method. The terms that were evaluated explicitly in time were discretized by using the third-order Adams-Bashforth method for the momentum equations and the Euler forward-in-time method for the transport equations.

A native transport sub-model for passive tracers (Passive TRACERS -`PTRACERS`- package; according to the MITgcm's jargon, a passive tracer is a generic tracer that has no influence on the hydrodynamics -e.g., by changing the density and/or viscosity-) is included in the MITgcm code. This sub-model solves the first three terms on the RHS of Eq. (10) (transport of a generic passive tracer). This transport is calculated by adopting a direct space–time discretization method for the advection–diffusion part of the tracer equations and a nonlinear, third-order advection scheme with a Sweby flux limiter (Sweby, 1984) to avoid spurious oscillations in the model output fields. When employing the direct space-time method and the flux-limited schemes, the Euler forward time stepping is adopted rather than Adams-Bashforth.

Because of the different length scales, horizontal and vertical turbulent processes are treated separately and are solved by adopting a selected subset of several available parameterizations: in this study, we chose a mixed Leith-Smagorinsky scheme for the horizontal processes (second term on the RHS of Eq. (10)) and the K-profile parameterization (KPP, Large et al., 1994) for the vertical processes (third term on the RHS of Eq. (10)).

The packages that were enabled during compilation (`#define ALLOW_PACKAGENAME`) were the standard geophysical fluid dynamics packages of the MITgcm ("`gfd`": `MOM_COMMON`, `MOM_FLUXFORM`, `MOM_VECINV`, `GENERIC_ADVDIFF`, `DEBUG`, `MDSIO`, `RW`, `MONITOR`), the oceanic packages ("`oceanic`": `GMREDI` and `KPP`), and our specific selections (`TIMEAVE`, `CAL`, `EXF`, `OBCS`, `FLT`, `DIAGNOSTICS`, `PTRACERS` and `GCHEM`), including the coupling and long time-stepping packages (`BFMCOUPLER` and `LONGSTEP`), which are the core of this peculiar implementation.

This code was compiled onto a Linux cluster that was equipped with Intel Xeon Ivy Bridge processors by using both the native GNU compiler (gfortran with openmpi libraries) and the Intel compiler (ifort: Intel Composer XE 2013 SP1) and by adopting the optimization levels `-O3` and `-O2`, respectively. Overall, the model performance increased by approximately 10% when using the Intel compiler. The results in this paper were obtained using the Intel compiler with the optimization set to `-O2`. Further details on the custom model installation are available on the MITgcm's online documentation.

2.3 BFM

The Biogeochemical Flux Model (BFM) is an open source, modular Fortran90 numerical model that was designed to describe the dynamics of the major biogeochemical processes that occur in marine ecosystems (Vichi et al., 2015). The standard configuration of the BFM solves the cycles of carbon, phosphorus, nitrogen, silica, and oxygen in the water-dissolved phase and in the plankton, detritus, and benthic compartments. Plankton dynamics are parameterized by considering a number of plankton functional groups, each representing a class of taxa. The BFM's plankton functional groups are subdivided into producers (phytoplankton), consumers (zooplankton), and decomposers (bacteria). These broad functional classifications are further partitioned into functional subgroups to create a planktonic food web (e.g., diatoms, picophytoplankton, microzooplankton, etc.). The structure of the plankton functional types is modular and can be adapted to specific needs. In fact, the BFM's code is organized into several modules devoted to several plankton function types: `Phytodynamics` (for the phytoplankton functional types), `Mesozoodynamics` and `Microzoodynamics` (for the zooplankton functional types), and `PelBacDynamics` (for bacteria). The two modules `OxygenReaerationDynamics` and `PelChemDynamics` for the oxygen and carbonate system dynamics, respectively, complete the pelagic system (subroutine `PelagicSystemDynamics`). The interface routine `EcologyDynamics` manages the memory allocation of the biogeochemical state variables and derivatives, and the external information that is required to calculate the biological equations: temperature, salinity, presence of ice, wind, position of the cell with respect to the surface or bottom, and atmospheric CO_2 partial pressure. The code and a full description of the model equations and parameterizations are freely available at http://bfm-community.eu.

For this application, we adopted the version v2 (Lazzari et al., 2012, 2016; Teruzzi et al., 2013, Melaku Canu et al., 2015, Cossarini et al., 2015b), which can be downloaded upon request from the BFM-consortium.eu website (GNU GPL license). The current BFM version uses a zero-dimensional data structure for the biogeochemical state variables. The present BFM includes four components ($\mathbb{C}$, $\mathbb{N}$, $\mathbb{P}$, and $\mathbb{S}$); four phytoplankton groups; four zooplankton groups; one group each of bacteria, detritus, labile and semilabile organic matter; and additional variables, such as dissolved oxygen and alkalinity (Fig. 1). In addition, chlorophyll is solved as a prognostic variable according to the formulation of Geider et al. (1997), and the carbonate system is solved by using the OCMIP formulation (Melaku Canu et al., 2015, Cossarini et al., 2015b).

2.4 The coupler

In this coupling scheme, we adopted a modular approach by considering the high complexity of the two models that were employed. The size of the codes according to the SLOCCount tool (Wheeler, 2015) is approximately 400,000 code lines for the MITgcm and approximately 20,000 for the BFM. The coupler is a package that handles the interface (APIs) between the host code (MITgcm) and the BFM to solve Eq. (7-8) and to efficiently manage the matrices that contain the variables and tendencies shared by the two models and the flow of information among the different sub-model components.

The MITgcm-BFM coupling (Fig. 2) was achieved by upgrading a few routines of the MITgcm package `GCHEM` (GeoCHEMistry, details in appendix A), which handles the evolution of tracers, and by developing an additional package, `BFMCOUPLER`, which was specifically designed as the interface with the BFM model. The BFM is called by the MITgcm as an external library; therefore, the BFM was compiled separately using the same compiler used for the MITgcm (additional details on the compilation options and instructions are provided in Appendix A).

The `BFMCOUPLER` package (dashed box in Fig. 2) manages the initialization and memory usage of the BFM. This package also calls the BFM core routines and solves several processes that are not included in either model. The interfaces among the different components of the coupled model were designed so that the tracer transport sub-model (MITgcm `PTRACERS` package) uses the *u*, *v* and *w* components of the velocity and the horizontal and vertical diffusivities (K_H and K_V) from the hydrodynamic sub-model to compute the tendency due to the transport ($gTracer_{trsp}$). Furthermore, the transport sub-model must consider the boundary conditions along the open boundaries of the model domain $(OBC)_C$ and the surface fluxes, such as the mass transport associated with the evaporation minus the precipitation minus the runoff term $(EmPmR)_C$.

As an interface, the `BFMCOUPLER` manages the transfer of information that is required by the BFM from both the hydrodynamic and transport sub-models of the MITgcm, and provides the integration solver (a MITgcm package) with the biogeochemical surface and bottom forcing and the sink/sources terms originated from the BFM ($gTracer_{bio}$). The values of the tracers are derived from the transport sub-model. Moreover, the hydrodynamic sub-model supplies the temperature, salinity and photosynthetic active radiation (*PAR*) values as well as additional forcing parameters (presence of ice, wind speed and air partial pressure of CO_2) and information, such as the position of the specific grid cell within the water column (surface, intermediate or bottom), which activates specific processes (e.g., surface air-sea gas transfer or bottom sediment fluxes). Then, the BFM calculates the biological partial derivative of Eq. (10) (fourth term), and the `BFMCOUPLER` returns this term to the time integration package, which integrates the transport and biogeochemical derivative terms to solve Eq. (10). Certain information used by the BFM, such as the *PAR* and wind values, can be calculated directly from the internal variables of the hydrodynamic sub-model (such as short wave radiation (Q_{sw}) or other atmospheric fields) or managed from external sources.

2.4.1 Integration scheme, operator splitting and longstep options

We considered several coupling strategies according to the MITgcm's code structure (Fig. 3). Within each time step of the model integration, which is coded in the routine `FORWARD_STEP`, the MITgcm solves the hydrodynamic equations (Eq. 1-6) through several routines: `DO_ATMOSPHERIC_PHYS`, `DO_OCEAN_PHYS`, `DYNAMICS`, and `TEMP_INTEGRATE` and `SALT_INTEGRATE`; further adjustments for temperature and salinity (e.g., filters) are applied in `TRACERS_CORRECTION_STEP` (Adcroft et al., 2016).

Different options can be used to solve the evolution of tracers (Eq. 10), which can be controlled by the pre-compilation option "`gchem_separate_forcing`". When this option is false (`#ifndef` in Fig. 3), a direct integration scheme is adopted; therefore, the transport ($gTracer_{trsp}$) and biogeochemical ($gTracer_{bio}$) tendencies are calculated by using the same (current) values of the physical and biogeochemical variables:

$$C_{n+1} = C_n + \left(gTracer_{trsp}(C_n, \mathbf{v}_n) + gTracer_{bio}(C_n, \theta_n, S_n, f_C)\right)\Delta t \qquad (11)$$

where $\mathbf{v}$, θ, S and f_C are the hydrodynamic variables and the additional biogeochemical forcing and Δt is the time discretization, which is the same adopted by the hydrodynamic sub-model.

The biogeochemical tendency, which is solved by calling the BFM through the routine `BFMCOUPLER_CALC_TENDENCY`, is temporarily stored in the `gchemTendency` matrix, which is then summed to the overall tracer tendency, `gTracers`, in the routine `PTRACER_APPLY_FORCING`, along with the tendency term from the evaporation minus the precipitation effect (`surfPtracers`). The transport terms of the tracers (which update the `gTracers` matrix) are subsequently calculated within the `PTRACER_INTEGRATE` routine by several routines (`GAD_ADVECTION`, `GAD_CALC_RHS`, `IMPLDIFF` and others) according to the options and numerical schemes selected in the specific MITgcm simulation setup. The `TIMESTEP_TRACER` routine calculates the integration of Eq. (10) by providing a new state for the tracers. However, when the MITgcm setup is prescribed with an implicit vertical diffusion scheme, an update of the state of tracers is solved within the `IMPLDIFF` routine according to the specific parameterization of the vertical diffusion (e.g., KPP, GGL90). Finally, if open boundary conditions are prescribed in the MITgcm setup, the `OBCS_APPLY_PTRACER` routine applies the updated values of the tracers at the boundaries. The calculation of the derivative of the transport processes ($gTracer_{trsp}$) involves several MITgcm packages (`GENERIC_ADVDIFF`, `PTRACERS`, `GCHEM`, `OBCS`, `KPP`, and `EXF`) and options (choice of the advection scheme, viscosity and diffusivity coefficients, parameterization of surface dilution/concentration of tracers from evaporation, precipitation, and runoff), which are exhaustively described in the MITgcm documentation (Adcroft et al., 2016).

For the second coupling option, a operator splitting scheme is selected when "`gchem_separate_forcing`" is true (`#ifdef`). In this case, the biogeochemical tendency ($gTracer_{bio}$) is calculated after the state of the tracers has been updated by the transport equation terms. An intermediated value of the tracers, $\tilde{C}_{n+1}$, is passed to `BFMCOUPLER_CALC_TENDENCY` along with the values of the updated hydrodynamic variables (eq. 12).

$$\begin{cases} \tilde{C}_{n+1} = C_n + gTracer_{trsp}(C_n, \mathbf{v}_n)\cdot\Delta t \\ C_{n+1} = \tilde{C}_{n+1} + gTracer_{bio}(\tilde{C}_{n+1}, \theta_{n+1}, S_{n+1}, f_C)\cdot\Delta t \end{cases} \qquad (12)$$

This option allows for the development of an integration scheme with different time steps for the hydrodynamic and transport parts on one side and for the biological processes on the other.

A third option is an operator splitting algorithm, which involves the MITgcm package `LONGSTEP` (Adcroft et al., 2016) and adopts different time steps for the hydrodynamic and transport-biogeochemical components, thus increasing the computational performance of a coupled simulation. In particular, the tracer time step is set as a multiple (LS_n) of the main (hydrodynamic) time step, $\Delta t_{trc} = LS_n \cdot \Delta t$, whereas the terms $\mathbf{v}$, θ , S and f in Eq. (11) are replaced by suitable averages of the physical variables. The calculation of the averages is controlled by the parameter `LS_when_to_sample`, which defines the position within the code workflow in which the hydrodynamic variables are sampled (`longstep_average`, Fig. 3) and biogeochemical tracer tendencies are calculated (`LONGSTEP_THERMODYNAMICS`, Fig. 3). To activate this option, the `LONGSTEP` package code must be modified properly: the `LONGSTEP_THERMODYNAMICS` routine must be modified by adding a call to the modified `GCHEM_CALC_TENDENCY` routine.

This third method is preferred over the previous one as a possible method of decoupling the numerical biogeochemistry solution from the hydrodynamic solution. We tested the model to verify the trade-off between the increase in computational performance and the loss of accuracy in the model results as a function of the extension of the time step for the tracer equations (LS_n , see section 3.1.3).

2.4.2 `BFMcoupler` processes

The core of the present coupling scheme is the new routine `BFMCOUPLER_CALC_TENDENCY`, which is called by `GCHEM_CALC_TENDENCY` or by `GCHEM_FORCING_STEP`. The approach adopted in this coupling scheme is to loop in space and to call the BFM as a subroutine to calculate the derivative terms of each biogeochemical tracer for each computational grid point ($gTracer_{bio}$ in Fig. 2). The derivatives of the chemical and biological processes are calculated by the BFM model via an Euler forward scheme through the `BFM0D_ECOLOGY_DYNAMICS` routine (a BFM routine) and stored in the 4D MITgcm matrix `gchemTendency`. Additionally, the contributions of other processes, which are not explicitly coded in the BFM, are solved within `BFMCOUPLER_CALC_TENDENCY`, namely, the light penetration formulation, the sinking of phytoplankton and detritus, and the exchange processes in the surface and bottom layers of the water column.

In particular, the `BFMCOUPLER` package calculates the vertical profile of *PAR* along the water column, starting from the surface *PAR*, which is read from an external file or by using the shortwave radiation field (Q_{sw}), which is converted into *PAR* by a standard bulk formula, if the native MITgcm atmospheric forcing package `EXF` is active (Britton and Dodd, 1976):

$$PAR_s = Q_{sw} \cdot conv \cdot pfrac \qquad (13)$$

where PAR_s is the *PAR* at the sea surface, *conv* is a conversion factor of 4.6 µEin/m^2/s (W/m^2)$^{-1}$, and *pfrac* is the fraction of the radiation in the visible band, which equals 0.4. The calculation of *PAR* along the water column, Eq. (14), is performed in the cell centre according to the Lambert-Beer formulation for the light exponential decay with depth and the shading of detritus and phytoplankton:

$$PAR_z = PAR_s \cdot e^{-\int_0^z (K_{ext} + \sum_j Chl_j Kp_j + R_{\mathbb{C}}^{(3)} K_R) dz} \qquad (14)$$

where Chl_j is the chlorophyll concentration of the j^{th} phytoplankton functional type (PFTs), $R_{\mathbb{C}}^{(3)}$ is the carbon concentration of the detritus or optically active organic matter, and Kp_j and K_R are the corresponding extinction factors. K_{ext} represents a background value set constant and is equal to 0.035 m^{-1} (considering pure water), or it can be read from an external file. In the latter case, the external file contains maps of the background extinction factor, which can be built a priori to incorporate the contributions of different unparameterized processes (e.g., the pattern distribution of yellow substances).

`BFMCOUPLER` solves the sinking processes and is activated for the phytoplankton groups and detritus ($R_{\mathbb{C},\mathbb{N},\mathbf{P}}^{(3)}$ variables in Fig. 1):

$$\left.\frac{\partial C}{\partial t}\right|_{bio}^{sink} = w_s \frac{\partial C}{\partial z} \qquad (15)$$

where w_s is the sinking velocity (m s^{-1}), which is provided both as a constant value or as a diagnostic result produced by the BFM model based on the nutrient stress conditions of the phytoplankton cells (Lazzari et al., 2012). The equation is solved numerically based on an Euler forward scheme.

A second module of BFMCOUPLER was designed to easily handle the boundary conditions at the surface and bottom. At the surface, air deposition can constitute an important source of nutrients in oligotrophic systems. Furthermore, when the runoff and nutrient discharge from rivers cannot be incorporated into the MITgcm OBCS package (as in Cossarini et al., 2015a), incorporating these factors as external surface forcings may be necessary (i.e., as localized runoff). Therefore, such contributions are prescribed as additional terms in gchemTendency in the surface layer by reading time-varying 2D maps from external files:

$$\left.\frac{\partial C}{\partial t}\right|_{bio}^{surf} = flux_C\big|_{surf} \qquad (16)$$

The coupled MITgcm-BFM model includes a simple parameterization of the fluxes at the water-sediment interface, which includes the burial of detritus (e.g., a net export flux from the ecosystem) and an incoming flux of nutrients into the deepest cell of the water column. Burial is parameterized as the first-order kinetics of the carbon ($\mathbb{C}$), nitrogen ($\mathbb{N}$) and phosphorus ($\mathbb{P}$) contents in the detritus ($R^{(3)}_{\mathbb{C},\mathbb{N},\mathbb{P}}$ variables), which is exported out from the bottom grid cell:

$$\left.\frac{\partial R^{(3)}_{\mathbb{C},\mathbb{N},\mathbb{P}}}{\partial t}\right|_{bio}^{bottom} = -k_{burial} R^{(3)}_{\mathbb{C},\mathbb{N},\mathbb{P}} \qquad (17)$$

In the same grid cell, the nutrient (for C equal to $N^{(1)}$, $N^{(2)}$ and $N^{(3)}$ in Fig. 1) bottom fluxes are set either as a constant rate over the entire domain or as time-varying 2D maps that can be read from an external file or provided by the benthic module of the BFM (which is foreseen in an ongoing development of the model):

$$\left.\frac{\partial C}{\partial t}\right|_{bio}^{bottom} = flux_C\big|_{bottom} \qquad (18)$$

The BFMCOUPLER involves the use of several external surface forcing fields, such as the surface photosynthetic active radiation, background light extinction factor, sediment fluxes, and partial pressure of atmospheric carbon dixiode, which are used by the BFM to calculate the air sea CO_2 exchanges. These fields are managed by the BFMCOUPLER package through the BFMCOUPLER_FIELDS_LOAD routine, which is a specifically modified replica of the EXTERNAL_FIELDS_LOAD routine of the MITgcm (Adcroft et al., 2016). This reading of external fields is controlled by two parameters: the period of forcing (`forcingCycle`) and the frequency of external forcing (`forcingPeriod`), which are specified in the `BFMCOUPLER` namelist (additional details in the Appendix).

2.4.3 Compilation and set up

The MITgcm and BFM must be compiled with the same compiler. We tested the code by using both the GNU and Intel compilers on several HPC platforms. Here, we report the results obtained by running the model (compiled with Intel) on a Linux cluster. The BFM is compiled as an independent library by using the following option of the BFM `makefile`: `mkmf -p $BFM_LIB`, and by configuring the `config_BFM.sh` compiling bash script with the appropriate compilation options (modules, optimization, and compiler), which are also used for the MITgcm compilation. Then, the `build_option` file for generating the MITgcm `makefile` must be modified by adding the path to the BFM compiled library and include files. Additional details are given in the manual of the `BFMCOUPLER` package (Appendix A).

3 Results

We tested the new coupled hydrodynamic-biogeochemical model against two case studies: an idealized experiment (a cyclonic gyre in a mid-latitude closed domain) and a realistic configuration (central Mediterranean Sea). In the first case study, which was released along with the code and the manual (https://github.com/gcossarini/BFMCOUPLER), we aimed to test the coherence of the model with the expected dynamics based on theoretical considerations and to test the model's performance under different coupling configurations. The second application was not meant to produce a thoroughly validated description of the dynamics of the area but has been designed to show that the coupled model (once run in a realistic setup) can be used to investigate a wide range of processes from coastal areas to open ocean. A thorough quantitative validation of the Mediterranean model output and an exploration of the results for analyses on the biogeochemical dynamics in the area are beyond the scope of this paper.

3.1 Idealized case study

This experiment was based on a simplified case study that consisted of an idealized domain (2° × 2° × 280 m closed box) that was forced by steady winds and a seasonal cycle of surface heat (downward long-wave and short-wave radiation) and mass (precipitation) fluxes. The horizontal shear in the surface wind field maintained a permanent cyclonic gyre, whereas the surface heat fluxes acted on the thermohaline properties of the water column, inducing a yearly cycle (summer stratification – winter mixing). This simulation was run for several years to reach steady-state conditions (perpetual year simulation).

3.1.1 Numerical configuration

This domain was discretized by adopting a uniform grid spacing (1/32°) in the horizontal direction, creating 64 grid cells in both directions. All the peripheral grid points of the bathymetry were land points (closed box), whereas the bottom of the domain was a bowl-shaped pit. In the vertical direction, the model was composed of 30 layers with non-uniform thickness (from 1.5 to 21 m). The time step equalled 300 s. External forcing fields were introduced via the MITgcm-native `EXF` package. The meteorological forcing consisted of 9 surface fields, namely, the 2-m air temperature (`atemp`), 2-m specific humidity (`aqh`), 10-m zonal and meridional wind (`uwind`, `vwind`), precipitation (`precip`), long- and short-wave incident radiation (`lwdown`, `swdown`), air pressure (`apressure`) and surface runoff (`runoff`). The wind stress and total heat flux were calculated via standard bulk formulae. The experiment was designed with no open boundaries to verify the mass conservation of chemical elements and simulate the effect of free surface dynamics on the distribution of tracers in the surface layer, which can be important for certain processes, such as the effects of concentration and dilution on the carbonate system variables. We chose the pre-compilation option, which allows for the presence of mass sources/sinks of fluid in the domain (3-D generalization of the oceanic real-fresh water flux option: `#define ALLOW_ADDFLUID`). With this option enabled, the net contribution of precipitation, evaporation and runoff can be considered in the total mass budget. In particular, we activated the "exact conservation" of fluid in the free-surface formulation (`#define EXACT_CONSERV`) so that the temporal evolution of the free surface height exactly equalled the divergence of the volume transport. We allowed the use of the non-linear free-surface option so that the surface level thickness (`hFactor`) could vary with time (`#define NONLIN_FRSURF`). The tests were run by adopting the following runtime options (in the namelist "`data`") for the free surface formulation and the volume conservation constraints:

```
&PARM01
implicitFreeSurface=.TRUE.,
exactConserv=.TRUE.,
useRealFreshwaterFlux=.TRUE.,
selectAddFluid=1,
linFSConserveTr=.FALSE.,
nonlinFreeSurf=4,
&END
```

When configuring the options for the passive tracers package (`PTRACERS`), we set the concentrations of the tracers in the surface mass fluxes (evaporation minus precipitation minus runoff) to always equal zero (`PTRACERS_EvPrRn(tracer_number)=0.0`). We used the same advection scheme (3rd order and direct space-time with a Sweby flux limiter) for active and passive tracers (*tracer*`AdvScheme=33`). Biogeochemical variables were initialized with suitable vertical profiles for winter condition all over the domain. The `BFMCOUPLER` package was configured without external forcing both at surface and at the bottom for nutrients, so that a closed system is simulated and mass conservation is checked. *PAR* was converted from short wave radiation, and light extinction factor was calculated considering a background value (K_{ext} =0.035 m^{-1}) and the shading effect of phytoplankton groups. All details of this experiment along with namelists and input files are given in the Appendix A.

3.1.2 Results of the simulation

The model simulated a realistic cyclonic circulation with associated mesoscale variability from vertical thermohaline stratification and flow instability. Relatively well-mixed thermohaline conditions in the winter induced a more unstable cyclonic gyre with small-scale mesoscale eddies (Fig. 4a), whereas a more stable and energetic cyclonic circulation occurred from stratified thermohaline conditions in the summer (Fig. 4b).

Figure 5 shows the evolution of several physical properties and biological components within the central part of the gyre. The coupled model simulated the evolution of the thermocline and nutricline and the effect of winter vertical mixing on the temperature and nutrient profiles (Fig. 5a and b). Figure 5 also shows the formation of surface phytoplankton blooms during early winter (Fig. 5c), the formation of the deep chlorophyll maximum (DCM) during summer (as a trade-off between the light penetration and the depth of the nutricline), and the effect of the erosion of the stratification during autumn on the biogeochemical properties of the basin (deepening of mixing layer depth - MLD - Fig. 5a). Net primary production (NPP, contour plot in Fig. 5d) showed the highest values in the proximity of the DCM during spring, although high primary productivity was also simulated in the upper part of the water column, where the high level of irradiance stimulated carbon fixation, especially for small-sized phytoplankton groups (not shown), even in the presence of low phytoplankton biomass.

The region close to the DCM was the most active biological area, i.e., the concentrations of all of the living variables (small and mesozooplankton groups and bacteria; Figs. 5e and f) were the highest and the fluxes fuelled the so-called classic food chain (Legendre and Rassoulzadegan, 1995). Nevertheless, significant bacterial biomass was also simulated in the upper part of the water column, where bacteria consumed the labile organic matter, which was side-produced by phytoplankton in the well-lid upper levels. Small zooplankton (sum of micro- and heterotrophic nanoflagellate groups) took advantage of the bacterial biomass, triggering the so-called microbial food web (Legendre and Rassoulzadegan, 1995), which dominated the upper part of the water column during summer. Oxygen (Fig. 5d) was higher in the upper part of the water column during winter because of the high level of NPP and the effect of re-aeration processes with the atmosphere. Bacterial production and the predominance of respiration over phytoplankton photosynthesis caused the autumn minimum.

3.1.3 Application of the longstep option

The computational cost of a 1-year simulation was approximately five hours when adopting an MPI configuration that featured 16 Ivy-Bridge cores. The code profiling (Fig. 6) indicated that most of the CPU time (i.e., up to 85%) was devoted to solve the differential equation for the high number of tracers (51). Solving the transport part ($Tracers_{trsp}$ in Fig. 6) of tracer equation (Eq. 10) accounted for 50% of the overall computational cost, whereas solving the biological part (Tracers$_{bio}$ in Fig. 6) accounted for 35%. The cost of solving tracer transport increased linearly with the number of tracers (e.g., Tracers$_{trsp}$ is almost 25 times larger than the time used to solve for temperature and salinity; Fig. 6), whereas the cost of the BFM calculations was primarily dependent on the solution of the carbonate system, although the complexity of the relationships among the biogeochemical variables (results not shown) was also a factor. The use of the MITgcm package `LONGSTEP` caused an almost exponential reduction in the computational cost for the integration of the tracer equation (Fig. 6). With a LS_n set to 8 (a time step for tracers, Δt_{trc}, equals 2400 s), the runtime was reduced by more than 80% with respect to the reference run. Assuming this optimization, the fraction that was devoted to the solution of the hydrodynamic and MPI routines accounted for 45%, whereas the remaining part (55%) was devoted to solving the transport-biogeochemical part. Within the tracer equation, 60% of the quota was allotted for transport and 40% of the quota was allotted for the BFM and the other biogeochemical processes.

The use of a coarser time resolution for the solution of the tracer equations implied errors with respect to the reference solution (Fig. 6). The errors were calculated as the root mean square of the difference of the integrated 0-200 m chlorophyll between the reference run (LS_n=1, i.e., no `LONGSTEP`) and the run with increased LS_n. The magnitude of the mean annual error increased almost linearly with the coarsening of Δt and equalled 0.0025 mg/m^3 at LS_n=8. Within a simulation, the largest differences between the reference run and the coarser time discretization run were registered during periods with the highest chlorophyll tendency, such as during autumn vertical mixing events along the entire water column and during the deep chlorophyll maximum formation in the spring (not shown). The errors became relevant (>0.01 mg/m^3) when larger values for LS_n (e.g., $LS_n \geq$10) were adopted.

3.1.4 Mass budget

The reference run was also used to verify the mass conservation of the coupled hydrodynamic-biogeochemical model by considering that the model configuration (i.e., non-linear free surface) was set to properly simulate the effects of free surface dynamics on the concentrations of the biogeochemical variables at the surface. Figure 7 shows the time series of the sea surface height (SSH) averaged over the entire basin. The results indicated the prevalence of rain over evaporation for the first part of the year and vice versa from May to October. For example, the evolution of variable alkalinity, which is a key parameter for resolving carbonate systems in oceans (Follows et al., 2006), within the surface layer was correctly anti-correlated with the derivative of SSH because the effects of concentration and dilution at the surface are dependent on the water mass balance. This model feature was provided along with the mass conservation capability for tracers (Fig. 7). The errors in mass conservation over time were small ($O(10^{-9})$) and they were caused by the computation of the time average of the model output. The coupled MITgcm-BFM model, which was configured with the non-linear free surface option, allowed us to efficiently simulate the dilution-concentration dynamics while preserving the ability to calculate the budget of the chemical elements with a high level of accuracy. This feature is indeed important considering the dynamics of variables like alkalinity, whose spatial patterns at the surface were dominated by the regional-spatial-scale distribution of the water mass budget (Cossarini et al., 2015b).

3.2 Adriatic-Ionian system case study

The coupled model was also used to simulate a realistic domain: the central Mediterranean Sea. This area, which encompasses the Adriatic and Ionian Seas (Fig. 8), was chosen because it is characterized by a wide range of interconnected ecosystems that span coastal areas, which are influenced by river discharges, and offshore regions, which are characterized by open-sea dynamics. Indeed, the northern part of the Adriatic is a continental shelf area influenced by terrestrial input (Solidoro et al., 2009, Cossarini et al., 2015a). This area is a site of dense water formation (Gačić et al., 2001, Querin et al., 2013) and represents one of the most productive areas of the Mediterranean Sea (Mangoni et al., 2008). The southern Adriatic Sea is characterized by an almost permanent geostrophic gyre modulated by deep winter mixing episodes (Gačić et al., 2002, Bensi et al., 2014), and it is connected to the Ionian Sea via the Otranto Strait. The Ionian Sea is the deepest sub-basin of the Mediterranean, and it is characterized by basin-scale circulation patterns and smaller mesoscale eddies. This sea is influenced by oligotrophic and salty waters originating from the Levantine basin and by the relatively fresh Atlantic water masses that flow from the west. The hydrodynamics of the area have been simulated by the Adriatic-Ionian implementation of the MITgcm (ADriatic IOnian System model (ADIOS), Querin et al., 2016), which we used in this study. The aim of this experiment is to show the ability of the new coupled model to properly simulate the effects of hydrodynamics on biogeochemistry within a wide range of oceanographic and ecological processes that span from a few kilometres to hundreds of kilometres and from oligotrophic to high-level trophic conditions.

3.2.1 Domain and model setup

The model domain was delimited by the Sicily channel (Lon 12.2 E) on the western side and by the Cretan Passage (Lon 22.7 E) on the eastern side. The Strait of Messina and the Gulf of Corinth were excluded in this study. The horizontal resolution was 1/32° (approximately 3 km), whereas the vertical grid consisted of 72 z-levels; therefore, the ADIOS model could be easily nested into the 1/16° Copernicus Mediterranean Modelling Forecasting system (CMEMS MED-MFC; Lazzari et al., 2010), which shares the same bathymetry along the open boundary of ADIOS.

The model setup only considered the main rivers that flow into the Adriatic Sea, whereas the minor contributions that flow into the Ionian Sea were neglected. River contributions were introduced as local boundary conditions, imposing observed daily fresh water flow rates for the major rivers (e.g., Po) and climatological annual flow rates for the others, with spring and autumn maxima and winter and summer minima (Querin et al., 2013, Janeković et al., 2014). The tracer concentrations at the river mouths were constant in space and time (Table 1), and the mass fluxes were calculated by multiplying the concentrations by the flow rate of each river.

The boundary conditions along the Sicily Channel and along the Cretan Passage were derived from the CMEMS MED-MFC system (Tonani et al., 2008, Lazzari et al., 2010) for both the hydrodynamic and biogeochemical variables (*OBC* and $(OBC)_C$ in Fig. 2). The output of the 1999-2012 reanalysis (Salon et al., 2015) was downloaded from the web portal marine.copernicus.eu. The present model configuration adopted a finer horizontal resolution (from 1/16° to 1/32°) with respect to the CMEMS MED-MFC system, whereas the vertical spacing was the same; hence, interpolating/extrapolating the hydrodynamic and biogeochemical fields in the vertical direction was unnecessary. Furthermore, both the CMEMS MED-MFC system and ADIOS adopted the BFM biogeochemical model; therefore, changes or conversions to the biogeochemical variables were not required. The initial conditions for the hydrodynamic and biogeochemical variables were also derived from the CMEMS MED-MFC system by linearly interpolating the original fields from 1/16° to 1/32°. Additional details on the ADIOS model setup are provided by Querin et al. (2016).

Surface meteorological forcing was derived from the Regional Climate Model (RegCM) developed at the International Centre for Theoretical Physics (ICTP) in Trieste. We used the 12-km horizontal resolution version with 3-hr output frequency (as in Querin et al., 2016). The heat fluxes (Q_θ in Fig. 2) at the air-sea interface were calculated using standard bulk formulae (via the MITgcm native `EXF` package); the air temperature, specific humidity, precipitation, incoming radiation and wind speed values were interpolated from the meteorological model; and the sea surface temperature was provided by the oceanographic model. The 3-hr temporal resolution can highlight the daily variability in the physical and biogeochemical properties of the uppermost layers of the water column (daily cycling of the *PAR*, temporal variability in the temperature and wind).

The specific settings for the `BFMCOUPLER` package were specified as follows. The background water light extinction factor was set considering a longitudinal negative gradient according to Lazzari et al. (2012) and the coefficient for the self-shading effect was set to 10^{-3} and 8×10^{-3} m^2 mg^{-1} chlorophyll for diatoms and the other three phytoplankton groups, respectively. The nutrient surface forcing (air deposition) was set to 0.00096 and 0.057 mmol m^{-2} d^{-1} for phosphorus and nitrate, respectively (Lazzari et al., 2012 and reference therein), whereas we assumed that the atmospheric carbon dioxide (pCO_2^{atm}) linearly increased from 380 to 395 in the period 2006-2012 according to the trend that was reported in Artuso et al. (2009). No bottom forcing was prescribed for the biogeochemistry.

3.2.2 Results of the simulation

The simulation covered the period from January 2006 to December 2012 at a time step of 200 s. In the following analysis, we disregarded the first 2 years of the simulation, which we considered a spin-up period for the biogeochemical variables from the CMEMS's coarser resolution fields. The MPI domain decomposition consisted of 16 × 14 subdomains run on 224 Intel Xeon Ivy Bridge cores of a Linux cluster, and the computational cost of the simulation was 65.8 hr per year. The runtime was significantly reduced by adopting the `LONGSTEP` option (Table 2). The wall clock time progressively decreased by increasing the longstep factor (LS_n) from 1 to 9. Then, time steps that were higher than 30 minutes substantially decreased the accuracy without further reducing the computational cost (Table 2).

We present the results for the ADIOS case study to demonstrate the ability of the new MITgcm-BFM coupled model to investigate closely interconnected hydrodynamic and biogeochemical processes for both coastal and open sea ecosystems.

On the western coastal areas of the Adriatic Sea, the maps in Figure 9 correctly display the patterns of low salinity, southward currents, high nitrate and chlorophyll concentrations, and strong primary production, which are all typical fingerprints of the Western Adriatic Current (WAC) system in the Adriatic Sea. The effect of the input from the northern rivers and the basin-scale cyclonic circulation generates a frontal system along the Italian coast. As is commonly observed in satellite chlorophyll maps (Barale et al., 2008), the width of the WAC frontal system decreases southwards, whereas weaker recirculation patterns are also visible in the central Adriatic Sea (Fig. 9). Other river-influenced coastal areas are simulated along the south-eastern areas of the Adriatic Sea, where the input from the Neretva and other south-eastern rivers triggers small-scale chlorophyll-a signals along those areas, as reported by Marini et al. (2010). The northward flow of salty and oligotrophic water, which enters through the Otranto Strait, confines the river's fertilization to a narrow coastal strip.

The coastal to open-sea gradients of nutrients were accurately simulated by the coupled model. As an example, Figure 9 shows that the nitrate patterns display a longitudinal gradient along the Adriatic and northern Ionian seas, and these results are consistent with the current climatologies (Cossarini et al., 2012, Solidoro et al., 2009, Zavatarelli et al., 1998). In the open-sea area of the Ionian Sea, the surface circulation is dominated by large mesoscale structures and a basin-scale anticyclone in the middle, and the downwelling area is characterized by minimal nitrate and chlorophyll concentrations (Fig. 9). This pattern is consistent with the climatology of Manca et al. (2004), even if the nitrate concentrations are slightly higher in the eastern Ionian Sea, which is related to overestimated eastern boundary values.

If we focus on the open-sea sub-surface dynamics, we can analyse how vertical processes affect the biogeochemistry. The vertical profiles of chlorophyll and phosphate for the two sites in Fig. 8 are depicted in Fig. 10. One site is located in the centre of the southern Adriatic gyre, which is characterized by strong winter vertical mixing, whereas the second is located in the centre of the large anticyclonic gyre in the Ionian Sea. A comparison between the two sites shows the ability of the coupled model to simulate the different regimes in the two areas. The southern Adriatic Sea presents a much higher mixed layer depth in winter, a shallower nutricline than the Ionian Sea, more intense inter-annual variability in the cyclic alternation of winter vertical mixing phases, and the onset of summer stratification.

The intense vertical mixing in the southern Adriatic area during winter drives the upwelling of nutrient-rich water, which contributes to a shallow nutricline (up to the depth of the DCM) during summer. However, winter ventilation in the Ionian Sea's open areas rarely reaches a depth of 250 m; consequently, nutrient-rich water remains confined to the deepest layers (below 200 m). The two areas are characterized by different biological regimes because of the different depths of the nutricline and the superimposed longitudinal gradient of the background light extinction factor (according to Lazzari et al., 2012).

Another interesting coupled hydrodynamic-biogeochemical feature is displayed along the southern coast of Sicily, where the entrance of modified Atlantic water (MAW, low-saline water mass in Fig. 9a) and the simulated coastal upwelling from westerly winds, induce vertical transport of nutrients, consistent with the findings of Patti et al. (2010) and Rinaldi et al. (2014). Intense vertical dynamics trigger the high concentrations of nutrients and chlorophyll and the strong primary production simulated in the upper layer of the northern Sicily channel (Fig. 9b), and these results are consistent with the typical patterns observed in satellite chlorophyll maps (Volpe et al., 2012).

The computation and diagnostics of the transport components for the tracers (e.g., zonal and meridional advection and diffusion, vertical advection and implicit and explicit diffusion) are already implemented in the native `PTRACERS` and `DIAGNOSTIC` packages of the MITgcm. This feature, which is complemented by the ability to calculate the surface and lateral fluxes at the boundaries through the `BFMCOUPLER` package, allows us to calculate the budget of the simulated chemical elements in marine ecosystems. As an example, we evaluated the meridional transport across the Otranto Strait for the carbon components along with other fluxes at the domain interfaces (i.e., the CO_2 flux at the air-sea interface and the river input) to calculate the carbon budget in the Adriatic Sea. The results show that the Adriatic Sea acts as a downwelling pump of carbon for the Mediterranean Sea. In particular, the Adriatic Sea imports carbon from rivers (3.17 10^{12} g$_{\mathbb{C}}$ y^{-1}) and from the atmosphere (1.65 10^{12} g$_{\mathbb{C}}$ y^{-1}). At the Otranto Strait, the Adriatic Sea imports carbon through the surface layer (0-200 m): 192.7 10^{12} g$_{\mathbb{C}}$ y^{-1} in terms of dissolved inorganic carbon (DIC) and 0.2 10^{12} g$_{\mathbb{C}}$ y^{-1} in terms of organic carbon. Conversely, this sea exports carbon through the bottom layer (200-1000 m): 197.7 10^{15} g$_{\mathbb{C}}$ y^{-1} and 0.03 10^{15} g$_{\mathbb{C}}$ y^{-1} in term of DIC and organic carbon, respectively. Finally, the Adriatic Sea is a net sink (approximately 4.7 10^{12} g$_{\mathbb{C}}$ y^{-1}) of carbon into the interior of the Mediterranean Sea. In terms of the transport across the Otranto Strait, Figure 11 shows the complex structure of the northward (red) and southward (blue) fluxes simulated by the coupled model. In particular, organic carbon (sum of all the living components: $P_{\mathbb{C}}^{(1,2,3,4)}$, $Z_{\mathbb{C}}^{(1,2,3,4)}$ and $B_{\mathbb{C}}^{(1)}$; and detritus, $R_{\mathbb{C}}^{(3)}$) is mainly confined to the surface layer for both the inflow and outflow. A barely visible flux of organic carbon toward the Ionian Sea is depicted along the western slope below a depth of 200 m (mainly because of the sinking of detritus). The northward and southward fluxes of DIC along the surface (Fig. 11) are characterized by the same organic carbon pattern and nearly balanced. Additionally, an outflow (blue) area at a depth of 300-900 m along the left flank of the strait indicates DIC transport associated with the Adriatic Dense Water Outflow Current (DWOC, Gačić et al., 2001). This carbon flux represents the export term that closes the budget of the Adriatic Sea and replenishes the layer of the Ionian Sea below the depth of the Levantine Intermediate water, which suggests a possible mechanism for the long-term carbon sequestration in the Mediterranean Sea.

4 Discussion and conclusion

In this paper, we presented a coupling between two widely used models, the MITgcm and BFM, and we showed the potential of the new coupled model. These two models were developed by two different scientific communities that are actively and constantly involved in improving the codes. When one model is directly embedded into another, code developments might represent an issue because of the constant and tedious work of keeping one code updated with respect to the other. Therefore, the coupling in this paper was designed to preserve the independence of the two models as much as possible. The number of modifications that were required for the two original codes was limited, and changes could be easily managed should each single model be upgraded. In our solution, the MITgcm remained the host code, the BFM was compiled and linked as an independent library, and the new `BFMCOUPLER` package handled all the coupling procedures and concentrated all the coding effort. The upgrades to the MITgcm enumerated less than 10 new code lines in a few routines (in the `GCHEM` and `LONGSTEP` packages) and the list of available diagnostics (in the `DIAGNOSTIC` package). On the BFM side, several "include" files contained a list of newly added variables. The order of the variables in the BFM's include files and in the MITgcm's file `data.ptracer` must be consistent (see Appendix A). This feature is important because the BFM (Vichi et al., 2015) can be customized in terms of both the number of state variables and processes, thus increasing the flexibility of the new coupled model for a wider range of applications.

Despite the growth of computational resources, the efficiency of coupled codes can be still an issue because of the large size of the computational grids (Blom and Verwer, 2000). Domain decomposition and parallelization tools are available in several coupling environments (e.g., FABM, Bruggeman and Bolding, 2014; and MESSy, Jöckel et al., 2008). Likewise, our coupling scheme has been thought to fully exploit the parallelization efficiency of the MITgcm (Marshall et al., 1997), and no additional coding effort (in terms of parallelization) is required by the users.

Other biogeochemical models of various complexity have already been embedded into the MITgcm (Dutkiewicz et al., 2009; Hauck et al., 2013; Cossarini et al., 2015a). Nevertheless, the BFM in this new coupled model has a biological complexity and a number of features (Lazzari et al., 2016) that increase the attractiveness of the model for many marine applications.

The MITgcm-BFM coupling scheme was primarily designed by considering the direct integration scheme because this framework has the highest level of numerical accuracy. The use of the `LONGSTEP` option reformulated the coupling as an operator splitting algorithm that allows for different time steps for hydrodynamics and coupled transport-biogeochemistry at the cost of accuracy. When using the `LONGSTEP` option, the results (Fig. 6 and Table 2) show that the loss of accuracy remained negligible only for a limited increase in the tracer time step. Furthermore, the coupling framework could handle a separate solution of hydrodynamics and transport processes from the biogeochemical processes through the use of the `gchem_separate_forcing` option (Fig. 3). However, this approach would require a wider modification of the `GCHEM` package to introduce independent integration steps for the transport and biogeochemical parts of the tracers. Then, a more detailed analysis of the sensitivity (e.g., similar to what was proposed in Butenschön et al., 2012) of the biogeochemical model's results to the different coupling schemes and time steps should be performed for each specific application.

A direct integration scheme might be more appropriate for investigating the feedback of the biogeochemistry on the hydrodynamics of the system. An example is the calculation for the sinking of certain phytoplankton groups, which is a physical 1D process solved within `BFMCOUPLER` and related to the sinking velocity calculated by the BFM. Furthermore, the shading effect on light penetration caused by phytoplankton and other suspended matter currently only affects the *PAR* vertical profile (Eq. 14). However, this factor could be introduced as an extra term in the routine that calculates seawater thermodynamics (in the routines SWFRAC and EXTERNAL_FORCING). A new parameterization of the penetration of solar radiation could be used to estimate the biological effects on the seawater temperature, which might be an interesting issue in highly productive areas, such as the northern Adriatic Sea and the coastal strip along the Italian coast reached by the Western Adriatic Current (WAC). A realistic simulation of light absorption with depth could reduce the model errors when estimating temperature, which is affected by many other sources of uncertainty from the surface forcing data, the heat flux bulk formulation, the vertical resolution and the parameterization of vertical turbulent processes. The design of our coupler, which is characterized by the sharing of biogeochemical variables and their tendencies in the host model's memory structure, allows for the future implementation of the feedback effects of biology on hydrodynamics.

Furthermore, the new coupling scheme was designed to foster development towards a full Earth system modelling approach, in which a wide range of processes among the Earth's spheres can be simulated online and the interactions and feedback effects can be directly considered. For example, the BFM has already been coupled with other ecosystem components (e.g., online coupling with the high-trophic-level model Ecopath with Ecosym, Akoglu et al., 2015). Moreover, the parameterization of Eq. (16) and (17) can be easily substituted by a call to a benthic model function, which solves the processes that occur in a single-layer sediment model and calculates the exchanges between the pelagic environment and the sediment.

Similarly, the MITgcm has already been coupled with atmospheric models. For example, the MITgcm has been coupled online with the atmospheric model RegCM in the Mediterranean Sea region (Giorgi et al., 2006) using the coupling framework OASIS (Artale et al., 2010). Therefore, our coupling scheme can act as a link between atmosphere-hydrosphere models and biosphere models. This coupler could be successfully used to study ocean-atmosphere interactions, such as the effects of climate scenarios on high-trophic-level ecosystem components or the feedback of ocean carbon pumps on the climate.

Finally, the results of the two test cases show that the new coupled model provides a realistic representation of a wide range of marine processes from costal to open-sea ecosystems, where the interplay of hydrodynamics and biogeochemistry is crucial. The effects of river plumes, coastal upwelling, and different vertical mixing regimes on phytoplankton dynamics were reasonably reproduced by the model and found to be consistent with both theoretical knowledge (Mann and Lazier, 2006) and published experimental findings for the Mediterranean Sea.

Acknowledgements

This study was partially funded by the Italian flagship project RITMARE. The authors thank Valentina Mosetti for the support.

Appendix A: Manual for the implementation and use of the BFMCOUPLERv1.0 package

A.1 Introduction

This package was developed as a specific interface among the MITgcm, the GCHEM package and the Biogeochemical Flux Model (BFM). The BFM (bfm-community.eu) is a complex and modular biogeochemical model that was designed to simulate multiple plankton functional types and the cycling of several chemicals (i.e., carbon, nitrogen, phosphorus, silica, and iron) within the marine pelagic ecosystem. BFMCOUPLER version 1.0 (v1.0) was designed to handle the application programming interfaces (APIs) between the MITgcm and BFM and to reproduce several processes (light extinction, sinking, and biogeochemical chemical fluxes at the air-sea and sea-bottom interfaces) that are not considered in both models. For more details regarding the equations, see section 2 of this paper.

A.1.1 General architecture of the coupled model

Several hydrodynamic-biogeochemical coupling options were implemented according to a previously implemented option in the GCHEM package. The gchem_separate_forcing option controls how and when the tracer tendencies are calculated and applied. The use of the LONGSTEP package is another coupling option available with BFMCOUPLER.

A.2 Key subroutines and parameters

A.2.1 Initialization

BFMCOUPLER_VARS.h contains the common blocks for the list of the BFM's state variables and diagnostic variables (BFM_var_list.h) and for the parameters and fields that are required to calculate the carbonate system solution, carbon dioxide air-sea exchange, *PAR*, light extinction, sinking and nutrient air deposition and bottom fluxes. Forcing fields can be initialized either with a background value by BFMCOUPLER_INI_FORCING.F or read from external fields. BFMCOUPLER_READPARAMS.F reads the namelist data.bfmcoupler, which contains the names of the files for the above fields. The parameters that manage the time intervals for reading, interpolating and applying the external forcings are read from the above namelist. The input namelist also contains specific parameters for the processes solved by BFMCOUPLER: sinking speed for detritus, self-shading coefficients for different phytoplankton groups, and background values of the seawater light extinction factor. The allocation of memory used by the BFM is set here by the BFM routine BFM_initialize. BFMCOUPLER_READPARAMS.F routine is called from the opportunely modified GCHEM_READPARAMS.F routine (a call statement to BFMCOUPLER_READPARAMS must be added). Accordingly GCHEM_INI_VAR.F must contain a call statement to BFMCOUPLER_INI_FORCING.F.

A.2.2 Forcings

The advection-diffusion tendencies of tracers are calculated in `ptracers_integrate.F`, whereas the biogeochemical process tendencies are handled by the routine `BFMCOUPLER_CALC_TENDENCY.F`, which is called from the opportunely modified `GCHEM_CALC_TENDENCY.F` (a `call` statement must be added), and controls the following:

- interface to the BFM routine `BFM0D_input_ecology` for the tracer values and all the necessary information used by the BFM itself (coordinates of the cells within the water column, temperature, salinity, *PAR*, pCO_2^{atm}, and wind speed in the corresponding surface grid point);
- call to the BFM model (`BFM0D_ecology_dynamics`);
- calculation of the *PAR*, the sinking of phytoplankton and detritus, and the atmospheric deposition of nutrients and bottom fluxes;
- interface from the BFM routine `BFM0D_output_ecology` for transferring and applying biogeochemical tendencies and diagnostics.

A.2.3 Loading fields

The external forcing fields used by the BFMCOUPLER (e.g., CO_2 air concentration, `PAR`, light extinction factor, nutrient air deposition, and bottom fluxes) are read by the routine `BFMCOUPLER_FIELDS_LOAD.F`, which is called from the opportunely modified `GCHEM_FIELDS_LOAD.F` (a `call` statement must be added). Input/output directives are based on the native MITgcm I/O package (`MDSIO`), a set of Fortran routines for reading and writing direct-access binary files .

A.2.4 Diagnostics

The `BFMCOUPLER` package uses the MITgcm's `DIAGNOSTICS` package. The definition of new specific diagnostics from the BFM's fluxes and variables is managed in `BFMCOUPLER_DIAGNOSTICS_INIT.F`, which is called from `BFMCOUPLER_INIT_FIXED.F`. The new diagnostics quantities are calculated in `BFMCOUPLER_CALC_TENDENCY.F` through a list of files (`BFMcoupler_VARDIAGlocal.h`, `BFMcoupler_VARDIAGcopy_fromD.h` and `BFMcoupler_VARDIAG_fill_diags.h`) that use the variables from the BFM routine `BFM0D_output_ecology` and specific instructions from the diagnostics package (`DIAGNOSTICS_FILL.F` routine).

New diagnostic quantities are listed in the namelist in the parameter file `data.diagnostics`, which specifies the frequency and type of output, the number of levels, and the names of all the separate output files.

The coupled MITgcm-BFM model can use a large number of tracers; therefore, increasing the `ndiagMax` parameter in `diagnostics_size.h` may be necessary. The initialization of `BFMCOUPLER` diagnostics is provided by adding a `call` statement to `BFMCOUPLER_INIT_FIXED.F` in the `GCHEM_INIT_FIXED.F` routine.

A.2.5 `LongStep`

The MITgcm package `LONGSTEP` allows the tracer time step to be longer than the time step used by the hydrodynamic model. When this package is activated along with the `BFMCOUPLER` package, a new specifically developed version of the routine `LONGSTEP_THERMODYNAMICS.F` has to be used. The new version of this routine includes a call to `BFMCOUPLER_CALC_TENDENCY`. The `BFMCOUPLER` routines use the hydrodynamic variables stored in the `LONGSTEP` variables, which are either the averages or temporal sub-samplings of the variables of the master hydrodynamic model depending on the `when_to_sample` parameter set in the `data.longstep` namelist file.

A.2.6 Compilation and compile time flags

The BFM is a Fortran95 code and must be compiled separately as an external library in advance (`$BFM_LIB/lib/libbfm.a`). According to the BFM's manual, a compiled library version is obtained by customizing the BFM `makefile` (`mkmf -p $BFM_LIB`). The `config_BFM.sh` compiling bash script must contain build options (modules, optimization options, and compiler) that are consistent with those of the MITgcm compilation.

When the MITgcm is compiled, the `build_options` file must be modified and the following lines must be added:

```
BFM_LIB=$BFM_PATH/lib
BFM_INC=$BFM_PATH /include
export LIBS="$LIBS'' –L $BFM_PATH/lib –lbfm
export INCLUDES="$INCLUDES -I$BFM_PATH /include"
```

The subroutines of the new package `BFMCOUPLER` must be included in the folder

`/MITgcm/pkg/BFMCOUPLER`,

which can be added to the original source tree of the code. `BFMCOUPLER` must be specified in the compile configuration file `packages_conf`.

Several specific compile time flags are set in `BFMcoupler_OPTIONS.h`:

`USE_QSW`: use Q_{sw} from the MITgcm to calculate the photosynthetic active radiation (*PAR*).

`READ_PAR`: read the *PAR* from a file set in `data.bfmcoupler`.

`USE_SHADE`: include the role of phytoplankton and detritus in the calculation of the vertical profile of the *PAR*.

`READ_xESP`: read the background light extinction factor from a file set in `data.bfmcoupler`.

`USE_SINK`: use the calculation for the sinking of phytoplankton and detritus.

`USE_BURIAL`: calculate the contribution of burial for detritus tendency at the bottom.

`USE_BOT_FLUX`: use input sediment fluxes for nutrients at the bottom.

`BFMCOUPLER_DEBUG`: activate a control on the tendencies calculated by the BFM.

A.3 Do's and Don'ts

This package must be run with both `PTRACERS` and `GCHEM` enabled. This package is configured for a number of biogeochemical variables specified by the BFM model. Therefore, `data.ptracers` must be configured accordingly (order of tracers equals what is specified in the `ModuleMem.F90` file from the BFM code). This package must also be run with diagnostics enabled.

A.4 Code availability and the experiment that uses `BFMCOUPLER`

The code can be downloaded from the https://github.com/gcossarini/BFMCOUPLER/tree/release-1.0 link (SHA-1 hash 02ce96dc), which corresponds to the version v1.0 described in the present manual.
The numerical experiment described in this paper (section 3.1) consists of an idealized domain forced by steady wind and a seasonal cycle of surface heat and mass fluxes. This case study simulates a permanent cyclonic gyre with a yearly cycle of thermohaline and biogeochemical properties. The input files along with the MITgcm and BFM namelists of the experiment are available at the https://github.com/gcossarini/BFMCOUPLER/input/ link. The modified MITgcm files, located in the /input/modified_MITgcm_files directory, should be linked, through the --mods option of the MITgcm builder (see section 3.4 of the manual) in order to override the original MITgcm source files with the modified ones, when the code is built.

Appendix B: List of symbols and variables used throughout the text

$\mathbf{C}$	biogeochemical tracers concentration [mmol m^{-3}] or [mg m^{-3}]
$\mathbf{v}_H = (u, v)$	horizontal (zonal (u) and meridional (v) component) of velocity, $\mathbf{v}$, [m s^{-1}]
w	vertical velocity [m s^{-1}]
ρ' and ρ_c	density anomaly and constant reference density [kg m^{-3}]
p and p'	pressure terms [N m^{-2}]
$\mathbf{F}_H$	horizontal forcing acting on momentum [m s^{-2}]
F_V	vertical forcing acting on momentum [m s^{-2}]
g	gravity acceleration [m s^{-2}]
f	Coriolis factor [s^{-1}]
ε_{nh}	non-hydrostatic parameter
k	unit vector in the vertical direction
Q_θ	forcing and dissipation terms for temperature [°C s^{-1}]
Q_S	forcing and dissipation terms for salinity [s^{-1}]
$\mathbf{Q}_C$	forcing terms for tracers [mmol m^{-3} s^{-1}]
Q_{sw}	short wave radiation [W m^{-2}]

$\mathbf{R}_{bio}$	biogeochemical reaction term [mmol m^{-3} s^{-1}]
PAR	photosynthetic active radiation [µEin m^{-2} s^{-1}]
K_H	horizontal diffusivity [m^2 s^{-1}]
K_V	vertical diffusivity [m^2 s^{-1}]
OBC	open boundary condition for hydrodynamics
EmPmR	evaporation minus precipitation minus run off [m^{-1}]
OBC_C	open boundary condition for tracers
$EmPmR_C$	evaporation minus precipitation minus run off for tracers
$gTracer_{bio}$	biogeochemical tendency of tracer equation [mmol m^{-3} s^{-1}], corresponding to *gchemTendency* in MITgcm nomenclature of Fig.3
$gTracer_{trsp}$	transport tendency of tracer equation [mmol m^{-3} s^{-1}]
wind	wind velocity [m s^{-1}]
ice	presence/absence of ice
Δt_{trc}	time step of the numerical solution for the biogeochemical terms when LONGSTEP is active [s]
LS_n	number of hydrodynamics time steps between tracer time steps
Δt	time step of the numerical solution [s]
pCO_2^{atm}	partial pressure of carbon dioxide in the atmosphere [ppm]
pCO_2^{sea}	carbon dioxide in the sea water [ppm]
DIC	dissolved inorganic carbon [mmol m^{-3}]
K_{ext}	background extinction coefficient for water [m^{-1}]
Kp_j	extinction coefficient of phytoplankton for j=1,4 [m^2 mg^{-1}]
K_R	extinction coefficient for detritus [m^2 mg^{-1}]
w_s	sinking velocity [m s^{-1}]
$P_{\mathbb{C}}^{(1,2,3,4)}$	carbon content of the four phytoplankton groups of BFM [mg m^{-3}]
$Z_{\mathbb{C}}^{(1,2,3,4)}$	carbon content of the four zooplankton groups of BFM [mg m^{-3}]
$B_{\mathbb{C}}^{(1)}$	carbon content of the bacteria of BFM [mg m^{-3}]
$R_{\mathbb{C}}^{(3)}$	particulate organic carbon of BFM [mg m^{-3}]

References

Adcroft, A., Campin, J.M., Dutkiewicz, S., Evangelinos, C., Ferreira, D., Forget, G., Fox-Kemper, B., Heimbach, P., Hill, C., Hill, E., Jahn, O., Losch, M., Marshall, J., Maze, M., Menemenlis, D. and Molod, A.: MITgcm user manual, MIT Department of EAPS, Cambridge, 479 pp, 2016.

Akoglu, E., Libralato, S., Salihoglu, B., Oguz, T. and Solidoro, C.: EwE-F 1.0: an implementation of Ecopath with Ecosim in Fortran 95/2003 for coupling and integration with other models. Geoscientific Model Development, 8(8), 2687-2699, 2015.

Artale, V., Calmanti, S., Carillo, A., Dell'Aquila, A., Herrmann, M., Pisacane, G., Ruti, P.M., Sannino, G., Struglia, M.V., Giorgi, F. and Bi, X.: An atmosphere–ocean regional climate model for the Mediterranean area: assessment of a present climate simulation. Climate Dynamics, 35(5), 721-740, 2010.

Artuso, F., Chamard, P., Piacentino, S., Sferlazzo, D.M., De Silvestri, L., Di Sarra, A., Meloni, D. and Monteleone, F.: Influence of transport and trends in atmospheric CO2 at Lampedusa. Atmospheric Environment, 43(19), 3044-3051, 2009.

Aumont, O., Ethé, C., Tagliabue, A., Bopp, L. and Gehlen, M.: PISCES-v2: an ocean biogeochemical model for carbon and ecosystem studies. Geoscientific Model Development, 8(8), 2465-2513, 2015.

Barale, V., Jaquet, J.M. and Ndiaye, M.: Algal blooming patterns and anomalies in the Mediterranean Sea as derived from the SeaWiFS data set (1998–2003). Remote Sensing of Environment, 112(8), 3300-3313, 2008.

Bensi, M., Cardin, V. and Rubino, A.: Thermohaline Variability and Mesoscale Dynamics Observed at the Deep-Ocean Observatory E2M3A in the Southern Adriatic Sea, in The Mediterranean Sea: Temporal Variability and Spatial Patterns (eds G. L. E. Borzelli, M. Gačić, P. Lionello and P. Malanotte-Rizzoli), John Wiley & Sons, Inc., Oxford, doi:10.1002/9781118847572.ch9, 2014.

Blom, J.G. and Verwer, J.G.: A comparison of integration methods for atmospheric transport-chemistry problems. Journal of Computational and Applied Mathematics 16, 381-396, 2000.

Britton, C.M. and Dodd, J. D.: Relationships of photosynthetically active radiation and shortwave irradiance. Agricultural Meteorology 17(1), 1-7, 1976.

Bruggeman, J. and Bolding, K.: A general framework for aquatic biogeochemical models. Environmental Modelling & Software, 61, 249-265, 2014.

Burchard, H., Bolding, K., Kühn, W., Meister, A., Neumann, T. and Umlauf, L.: Description of a flexible and extendable physical–biogeochemical model system for the water column. Journal of Marine Systems, 61(3), 180-211, 2006.

Butenschön, M., Zavatarelli, M. and Vichi, M.: Sensitivity of a marine coupled physical biogeochemical model to time resolution, integration scheme and time splitting method. Ocean Modelling, 52, 36-53, 2012.

Butenschön, M., Clark, J., Aldridge, J.N., Allen, J.I., Artioli, Y., Blackford, J., Bruggeman, J., Cazenave, P., Ciavatta, S., Kay, S. and Lessin, G.: ERSEM 15.06: a generic model for marine biogeochemistry and the ecosystem dynamics of the lower trophic levels. Geoscientific Model Development, 9, 1293-1339, 2016.

Cossarini, G., Solidoro, C., and Fonda Umani, S.: Dynamics of biogeochemical properties in temperate coastal areas of freshwater influence: lessons from the Northern Adriatic Sea (Gulf of Trieste). Estuarine, Coastal and Shelf Science, 115, 63-74, 2012.

Cossarini, G., Querin, S. and Solidoro, C.: The continental shelf carbon pump in the northern Adriatic Sea (Mediterranean Sea): Influence of wintertime variability. Ecological Modelling 314, 118-134, 2015a.

Cossarini, G., Lazzari, P. and Solidoro, C.: Spatiotemporal variability of alkalinity in the Mediterranean Sea. Biogeosciences, 12(6), 1647-1658, 2015b.

Crise, A., Allen, J.I., Baretta, J., Crispi, G., Mosetti, R. and Solidoro, C.: The Mediterranean pelagic ecosystem response to physical forcing. Progress in Oceanography, 44(1), 219-243, 1999.

Epicoco, I., Mocavero, S., Macchia, F., Vichi, M., Lovato, T., Masina, S. and Aloisio, G.: Performance and results of the high-resolution biogeochemical model PELAGOS025 within NEMO. Geosci. Model Dev., 9, 2115–2128, 2016.

Dutkiewicz, S., Follows, M.J. and Bragg, J.G.: Modeling the coupling of ocean ecology and biogeochemistry. Global Biogeochemical Cycles, 23(4), 2009.

Follows, M.J., Ito, T. and Dutkiewicz, S.: On the solution of the carbonate chemistry system in ocean biogeochemistry models. Ocean Modelling, 12(3), 290-301, 2006.

Gačić, M., Lascaratos, A., Manca, B.B. and Mantziafou, A.: Adriatic deep water and interaction with the Eastern Mediterranean Sea. In Physical Oceanography of the Adriatic Sea (pp. 111-142). Springer Netherlands, 2001.

Gačić, M., Civitarese, G., Miserocchi, S., Cardin, V., Crise, A. and Mauri E.: The open-ocean convection in the Southern Adriatic: a controlling mechanism of the spring phytoplankton bloom, Cont. Shelf Res., 22, 1897-1908, doi:10.1016/S0278-4343(02)00050-X, 2002.

Geider, R. J., MacIntyre, H. L., and Kana, T. M.: Dynamic model of phytoplankton growth and acclimation: responses of the balanced growth rate and the chlorophyll a: Carbon ratio to light, nutrient-limitation and temperature, Mar. Ecol.-Prog. Ser., 148, 187–200, 1997.

Giorgi, F., Pal, J.S., Bi, X., Sloan, L., Elguindi, N. and Solmon, F.: Introduction to the TAC special issue: the RegCNET network. Theor. Appl. Climatol. 86, 1–4, 2006

Haidvogel, D. B., Arango, H.G., Hedstrom, K., Beckmann, A., Malanotte-Rizzoli, P. and Shchepetkin, A.F.: Model evaluation experiments in the North Atlantic Basin: Simulations in nonlinear terrain-following coordinates, Dyn. Atmos. Oceans, 32, 239-281, 2000.

Hauck, J., Völker, C., Wang, T., Hoppema, M., Losch, M. and Wolf-Gladrow, D.A.: Seasonally different carbon flux changes in the Southern Ocean in response to the southern annular mode. Global biogeochemical cycles, 27(4), 1236-1245, 2013.

Heavens, N. G., Ward, D.S. and Natalie, M.M.: Studying and Projecting Climate Change with Earth System Models. Nature Education Knowledge, 4(5), 4, 2013.

Janeković, I., Mihanović, H., Vilibić, I. and Tudor, M.: Extreme cooling and dense water formation estimates in open and coastal regions of the Adriatic Sea during the winter of 2012, J. Geophys. Res. Oceans, 119, 3200–3218, doi:10.1002/2014JC009865, 2014.

Jöckel, P., Kerkweg, A., Buchholz-Dietsch, J., Tost, H., Sander, R. and Pozzer, A.: Technical note: coupling of chemical processes with the modular earth submodel system (MESSy) submodel TRACER. Atmos. Chem. Phys. 8 (6), 1677-1687, 2008.

Large, W. G., McWilliams J. C., and Doney C. S.: Oceanic vertical mixing: a review and a model with nonlocal boundary layer parameterization, Rev. Geophys., 32, 363–403, 1994.

Lazzari, P., Teruzzi, A., Salon, S., Campagna, S., Calonaci, C., Colella, S., Tonani, M. and Crise, A.: Pre-operational short-term forecasts for the Mediterranean Sea biogeochemistry, Ocean Sciences, 6, 25-39. doi:10.5194/os-6-25-2010, 2010.

Lazzari, P., Solidoro, C., Ibello, V., Salon, S., Teruzzi, A., Béranger, K., Colella, S. and Crise, A: Seasonal and inter-annual variability of plankton chlorophyll and primary production in the Mediterranean Sea: a modelling approach.Biogeosciences, 9, 217-233, doi:10.5194/bg-9-217-2012, 2012.

Lazzari, P., Solidoro, C., Salon, S. and Bolzon, G.: Spatial variability of phosphate and nitrate in the Mediterranean Sea: A modeling approach. Deep Sea Research Part I: Oceanographic Research Papers, 108, 39-52, 2016.

Legendre, L. and Rassoulzadegan, F.: Plankton and nutrient dynamics in marine water. Ophelia, 41, 153–172, 1995.

Ludwig, W., Dumont, E., Meybeck, M., and Heussner, S.: River discharges of water and nutrients to the Mediterranean and Black Sea: Major drivers for ecosystem changes during past and future decades?, Progr. Oceanogr., 80, 199–217, 2009.

Madec, G.: "NEMO ocean engine" (Draft edition r6039). Note du Pôle de modélisation, Institut Pierre-Simon Laplace (IPSL), France, No 27 ISSN No 1288-1619, 2014.

Manca, B., Burca, M., Giorgetti, A., Coatanoan, C., Garcia, M.J. and Iona, A.: Physical and biochemical averaged vertical profiles in the Mediterranean regions: an important tool to trace the climatology of water masses and to validate incoming data from operational oceanography. Journal of Marine Systems, 48(1),8 3-116, 2004.

Mangoni, O., Modigh, M., Mozetiˇc, P., Bergamasco, A., Rivaro, P. and Saggiomo, V.: Structure and photosyntetic properties of phytoplankton assemblages ina highly dynamic system, the northern Adriatic Sea. Estuar. Coast. Shelf Sci. 77,633–644, http://dx.doi.org/10.1016/j.ecss.2007.10.023, 2008.

Mann, K. H. and Lazier, J.R.N.: Dynamics of Marine Ecosystems, Blackwell Publishing, 496 pp., 2006.

Marini, M., Grilli, F., Guarnieri, A., Jones, B.H., Klajic, Z., Pinardi, N. and Sanxhaku, M.: Is the southeastern Adriatic Sea coastal strip an eutrophic area?. Estuarine, Coastal and Shelf Science, 88(3), 395-406, 2010.

Marshall, J.C., Adcroft, A., Hill, C., Perelman, L. and Heisey, C.: A finite-volume, incompressible Navier-Stokes model for the studies of the ocean on parallel computers, J. Geophys. Res., 102: 5753-5766, 1997.

Melaku Canu D., Ghermandi, A., Nunes, P.A., Lazzari, P., Cossarini, G. and Solidoro, C.: Estimating the value of carbon sequestration ecosystem services in the Mediterranean Sea: An ecological economics approach. Global Environmental Change. 32, 87-95, 2015.

Neumann, T.: Towards a 3D-ecosystem model of the Baltic Sea. Journal of Marine Systems, 25(3), 405-419, 2000.

Parekh, P., Follows, M.J. and Boyle, E.A.: Decoupling of iron and phosphate in the global ocean. Global Biogeochemical Cycles, 19(2), 2005.

Patti, B., Guisande, C., Bonanno, A., Basilone, G., Cuttitta, A., and Mazzola, S.: Role of physical forcings and nutrient availability on the control of satellite-based chlorophyll a concentration in the coastal upwelling area of the Sicilian Channel. Scientia Marina, 74(3), 577-588, 2010.

Polimene, L., Pinardi, N., Zavatarelli, M. and Colella, S.: The Adriatic Sea ecosystem seasonal cycle: Validation of a three-dimensional numerical model. Journal of Geophysical Research: Oceans, 111, C03S19, doi:10.1029/2005JC003260, 2006.

Querin, S., Cossarini, G. and Solidoro, C.: Simulating the formation and fate of dense water in a midlatitude marginal sea during normal and warm winter conditions. Journal of Geophysical Research: Oceans, 118(2), 885-900, 2013.

Querin, S., Bensi, M., Cardin, V., Solidoro, C., Bacer, S., Mariotti, L., Stel, F., and Malačič, V.: Saw-tooth modulation of the deep-water thermohaline properties in the southern Adriatic Sea, J. Geophys. Res.: Oceans. DOI: 10.1002/2015JC011522, 2016.

Rinaldi, E., Buongiorno Nardelli, B., Volpe, G. and Santoleri, R.: Chlorophyll distribution and variability in the Sicily Channel (Mediterranean Sea) as seen by remote sensing data, Continental Shelf Research, 77, 61-68, 2014.

Robson B. J.: State of the art in modelling of phosphorus in aquatic systems: Review, criticisms and commentary, Environmental Modelling and Software, 61, 339-359, 2014.

Salon, S., Cossarini, G., Lazzari, P., Teruzzi, A., Crise, A., and Solidoro, C.: Reanalysis of Mediterranean Sea biogeochemistry and the quest for biogeochemical seasonal forecasts in: Buch E., Antoniou Y., Eparkhina D., Nolan G. (Eds), Operational Oceanography for Sustainable Blue Growth. Proc. of the 7th EuroGOOS International Conference, 28-30 October 2014, Lisbon, Portugal. EuroGOOS publication, Brussels, Belgium, 2015. ISBN: 9789082479904.

Solidoro, C., Bastianini, M., Bandelj, V., Codermatz, R., Cossarini, G., Melaku Canu, D., Ravagnan, E., Salon, S., and Trevisani, S.: Current state, scales of variability, and trends of biogeochemical properties in the northern Adriatic Sea, J. Geophys. Res., 114, C07S91, doi:10.1029/2008JC004838, 2009.

Sweby, P.K.: High resolution schemes using flux-limiters for hyperbolic conservation laws. SIAM J. Num. Anal., 21 (5), 995–1011, doi:10.1137/0721062, 1984.

Teruzzi, A., Dobricic, S., Solidoro, C. and Cossarini, G.: A 3-D variational assimilation scheme in coupled transport-biogeochemical models: Forecast of Mediterranean biogeochemical properties, Journal of Geophysical Research: Oceans, 119(1), 200-217, 2013.

Tonani, M., Pinardi, N., Dobricic, S., Pujol, I., and Fratianni, C.: A high-resolution free-surface model of the Mediterranean Sea, Ocean Sci., 4, 1-14, 2008.

Vichi, M. and Masina, S.: Skill assessment of the PELAGOS global ocean biogeochemistry model over the period 1980–2000. Biogeosciences, 6(11), 2333-2353, 2009.

Vichi, M., Lovato, T., Lazzari, P., Cossarini, G., Gutierrez, Mlot E., Mattia, G., Masina, S., McKiver, W. J., Pinardi, N., Solidoro, C., Tedesco, L. and Zavatarelli, M.: The Biogeochemical Flux Model (BFM): Equation Description and User Manual. BFM version 5.1. BFM Report series N. 1, Release 1.1, Bologna, Italy, http://bfm-community.eu, pp. 104, 2015.

Volpe, G., Nardelli, B.B., Cipollini, P., Santoleri, R. and Robinson, I.S.: Seasonal to interannual phytoplankton response to physical processes in the Mediterranean Sea from satellite observations. Remote Sensing of Environment, 117, 223-235, 2012.

Wheeler, D. A.: SLOCCount software release 2.26, http://www.dwheeler.com/sloccount/, last access: 25 August 2015, 2015.

Zavatarelli, M., Raicich, F., Bregant, D., Russo, A., and Artegiani, A.: Climatological biogeochemical characteristics of the Adriatic Sea, J. Mar. Syst., 18, 227-263, 1998.

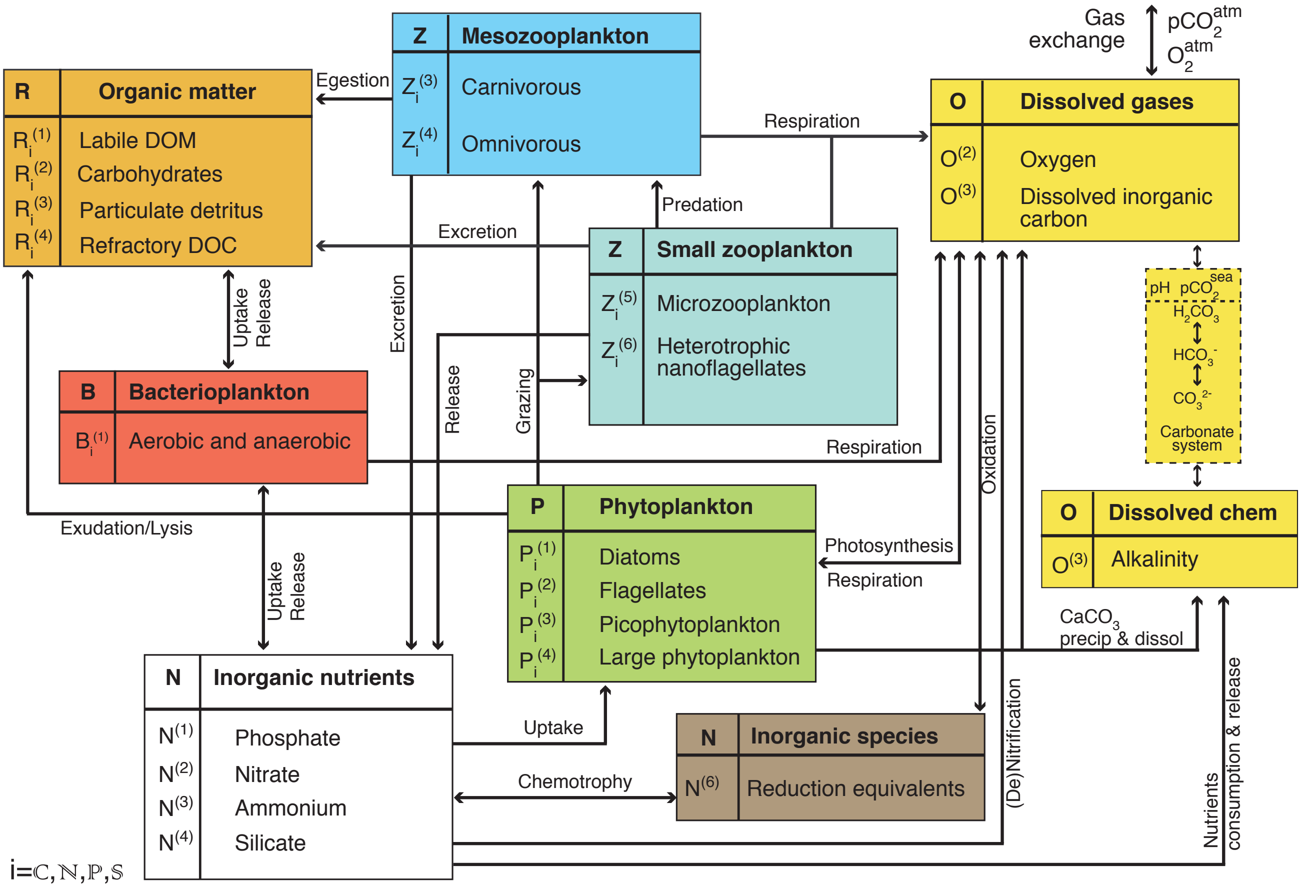

Figure 1: BFM model: scheme of the functional interactions among the variables in the version that was implemented in Lazzari et al. (2012), Melaku Canu et al. (2015), and Cossarini et al. (2015b). Variable names follow the BFM convention (Vichi et al., 2015). The subscripts indicate the chemical components (C: carbon; P: phosphorus, N: nitrogen, S: silica, O: oxygen).

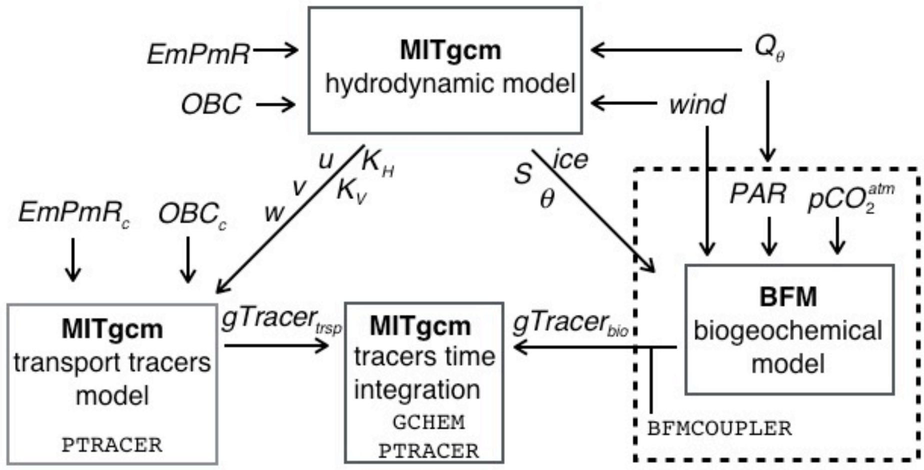

Figure 2: Description of the MITgcm-BFM coupling and interfaces among the different components of the coupled model.

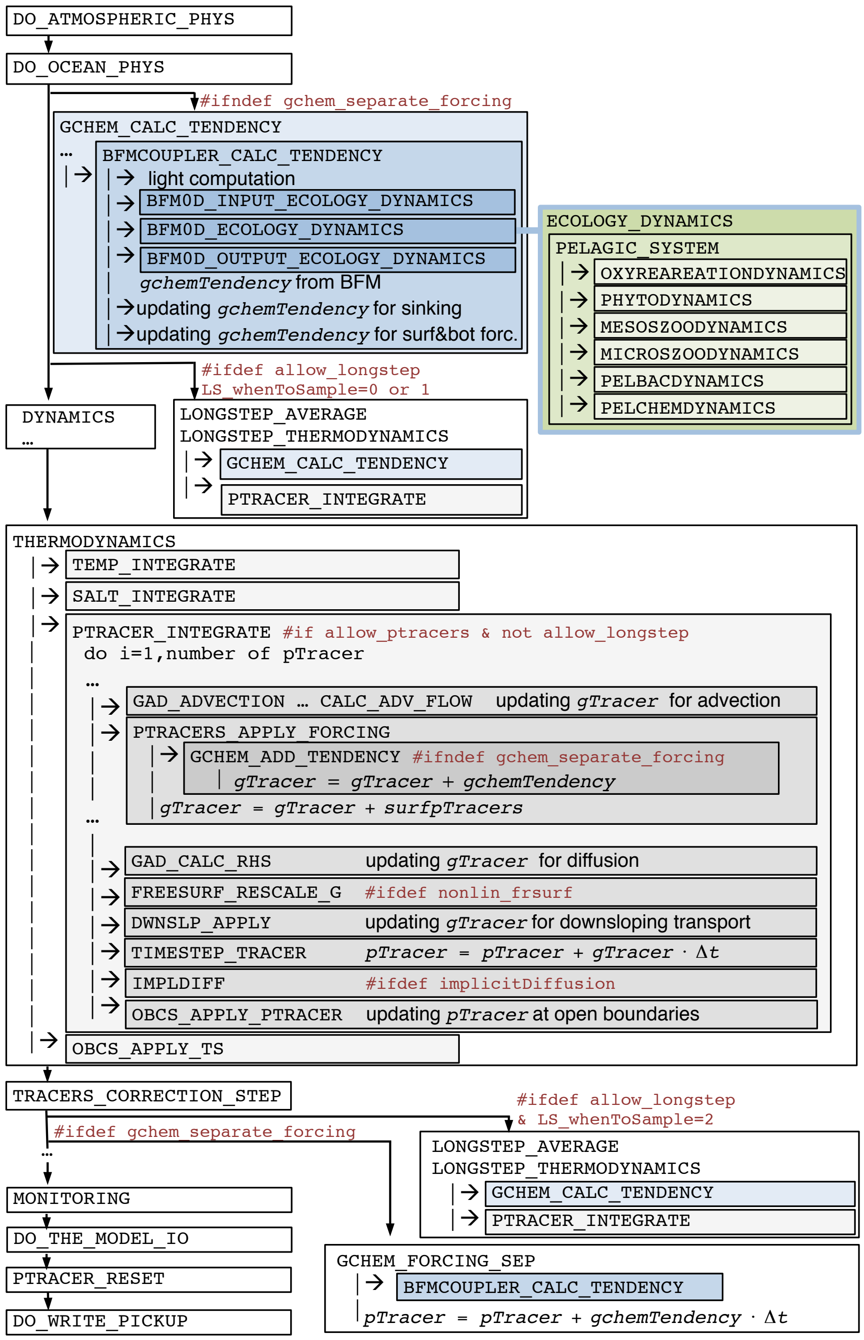

Figure 3: Workflow of the MITgcm routine `FORWARD_STEP`. The boxes indicate the routines and their dependencies. The matrix of the tracers' state variables (`pTracer`), the overall tendency of the tracer (`gTracer`), and the tendency for the biogeochemistry only (`gchemTendency`) are also specified. The blue boxes indicate modifications to either the MITgcm code or the `BFMCOUPLER` routines, whereas the green boxes indicate BFM routines. The pre-compilation options (#) and omitted parts (...) are also shown.

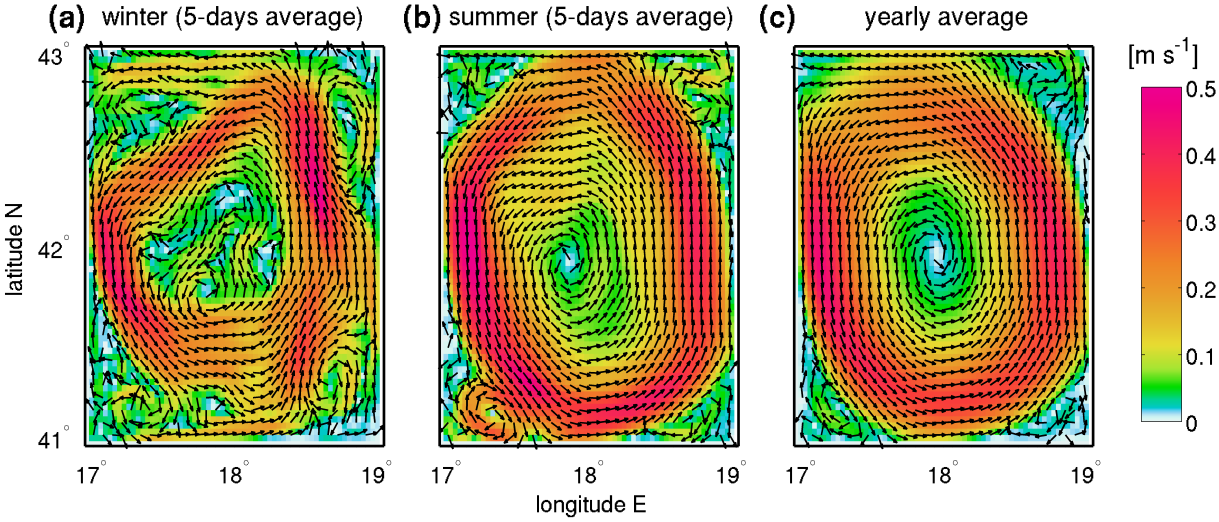

Figure 4: Idealized case study (circulation in a 2° × 2° × 280 m closed domain). Horizontal component of velocity: current speed (colour) and direction (vectors) at 12-m depth. 5-days average in winter (a) and summer (b), and yearly average (c).

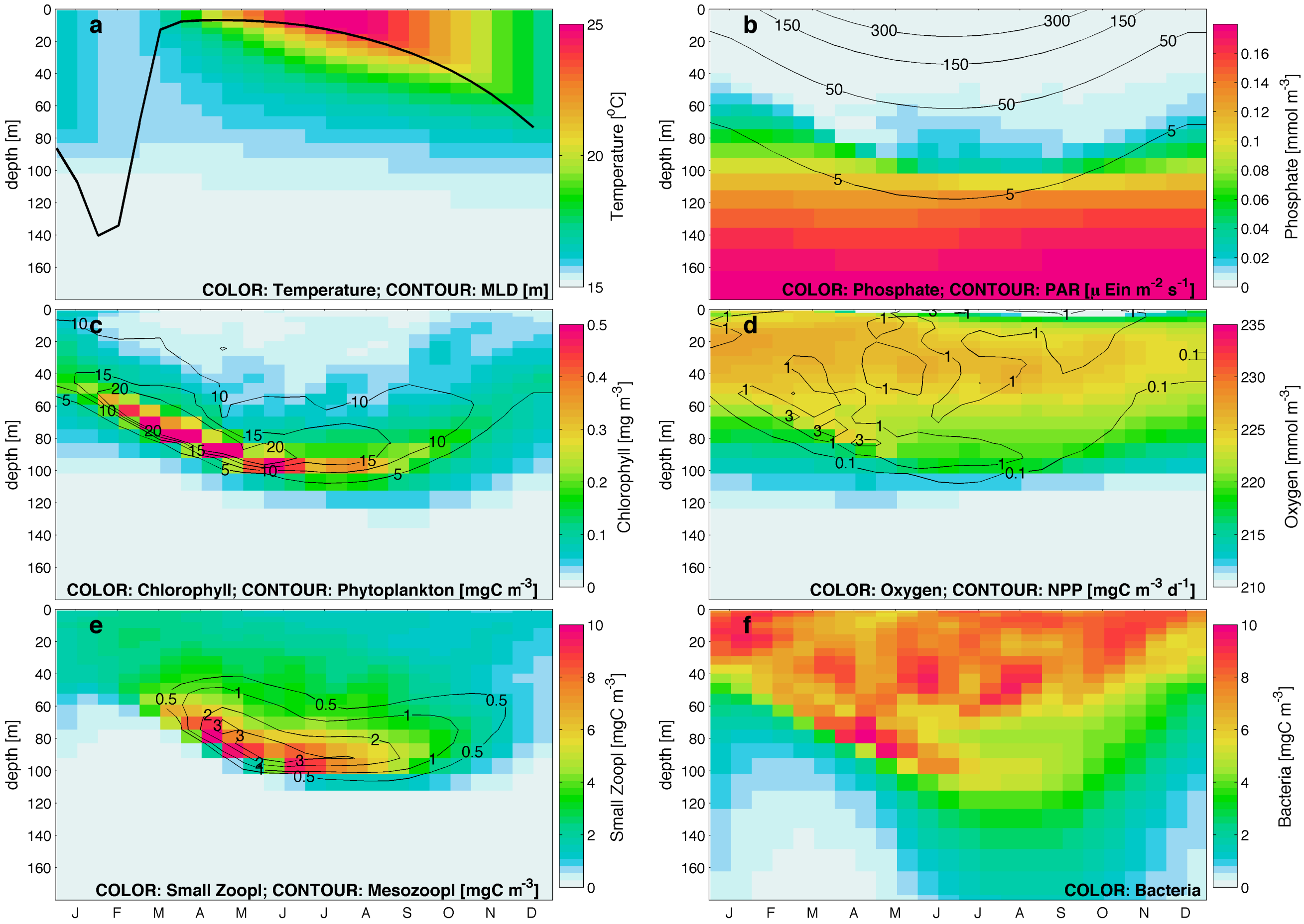

Figure 5: Hovmöller diagrams of the (a) Temperature and evolution of the mixed layer depth (MLD), (b) Phosphate and *PAR*, (c) Chlorophyll (sum of the chlorophyll content in the four phytoplankton functional groups) and Phytoplankton expressed in carbon biomass, (d) Oxygen and Net Primary Production (NPP), (e) Small Zooplankton (Small Zoopl) and Mesozooplankton (Mesozoopl), and (f) bacteria.

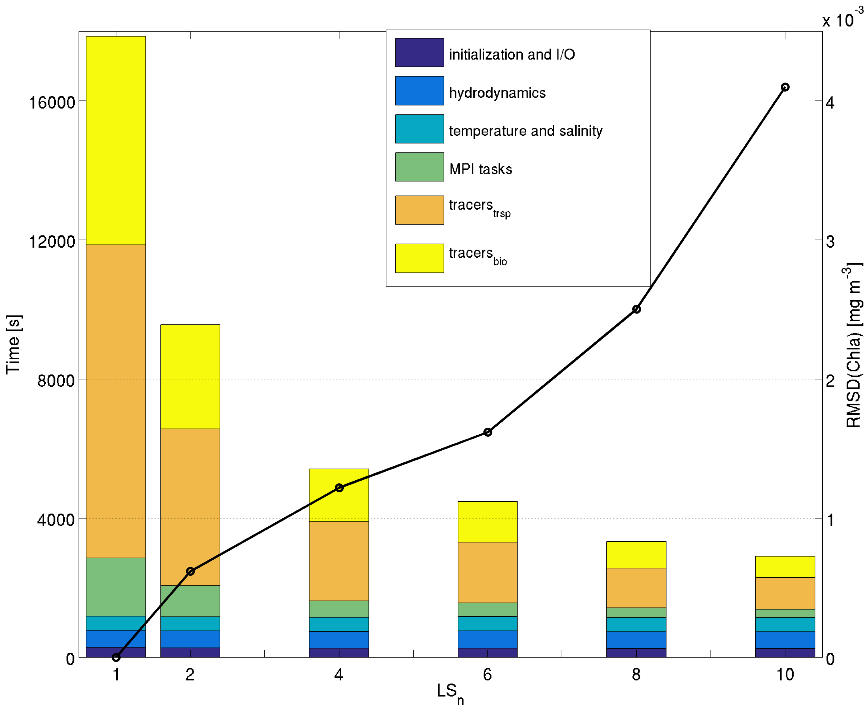

Figure 6: Wall clock time of the main MITgcm routines clustered in selected groups (left axes) as a function of the number of hydrodynamic time steps between tracer time steps (LS_n): initialization & I/O (sum of the routines: `MODEL_I/O`, `DO_STATEVARS_DIAGS`, `LOAD_FIELDS_DRIVER`, `MONITOR`, `DO_THE_MODEL_IO` and `DO_WRITE_PICKUP`), hydrodynamics (sum of `DYNAMICS`, `SOLVE_FOR_PRESSURE`, `INTEGR_CONTINUITY` and other routines); temperature & salinity (sum of the routines: `TEMP_INTEGRATE` and `SALT_INTEGRATE`); MPI tasks (`BLOCKING_EXCHANGES` routine); tracers$_{bio}$ (`GCHEM_CALC_TENDENCY`) and tracers$_{trsp}$ (`PTRACER_INTEGRATE`). The root mean square difference of the integrated chlorophyll (right axis) is shown as a function of LS_n .

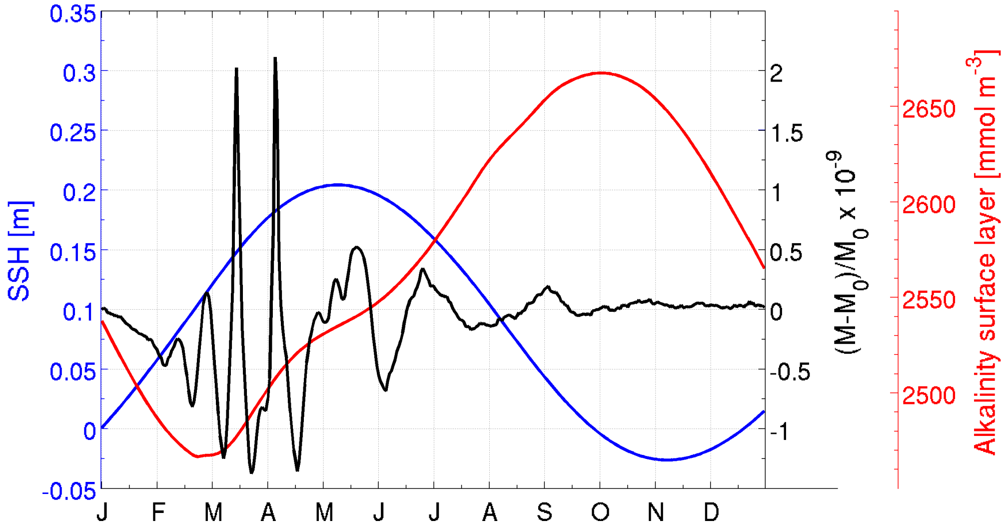

Figure 7: Evolution of SSH (blue line) and alkalinity (red line) at the surface layer together with the relative variation of total alkalinity mass (M) with respect to the initial condition (M0) over the whole domain (black line). The total alkalinity mass was obtained by multiplying the daily average model output by the domain volume, which included the time-varying SSH at the surface layer.

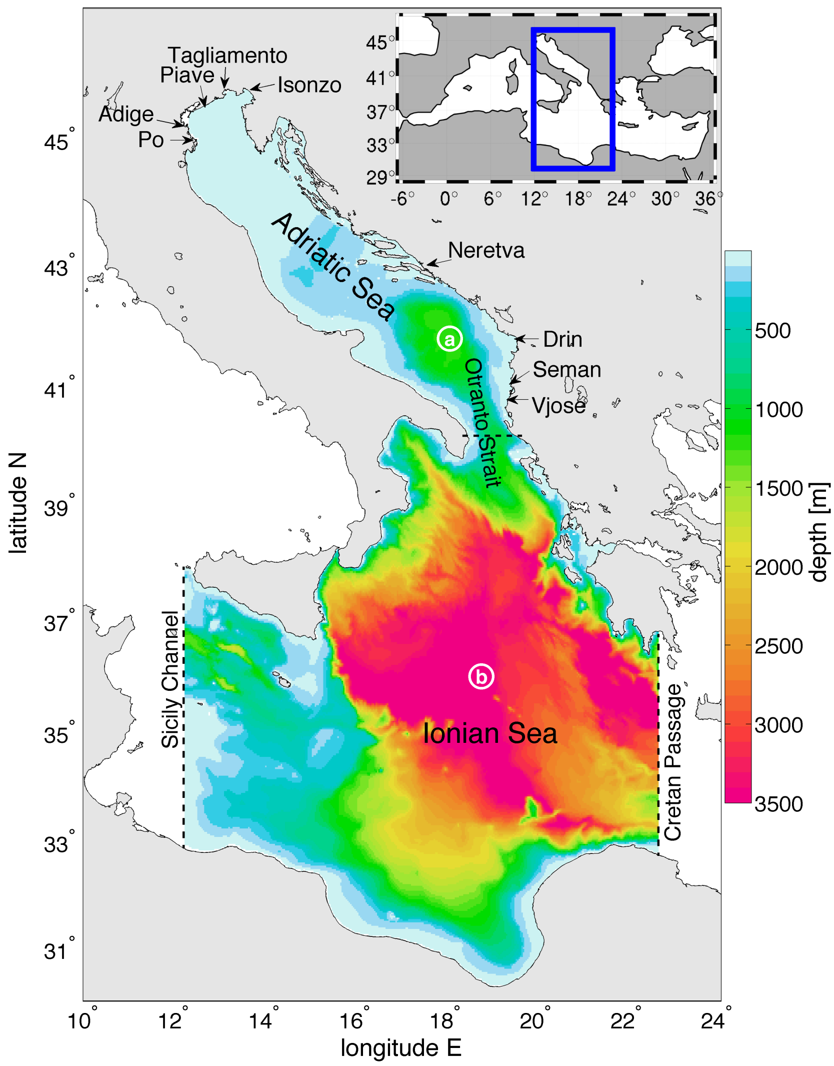

Figure 8: Bathymetry (depth in meters) of the Adriatic-Ionian model. The plot also indicates the location of the major rivers (arrows), the Otranto Strait and the position of the 2 sites (circles) that were selected to display the Hovmöller diagrams in Fig. 10.

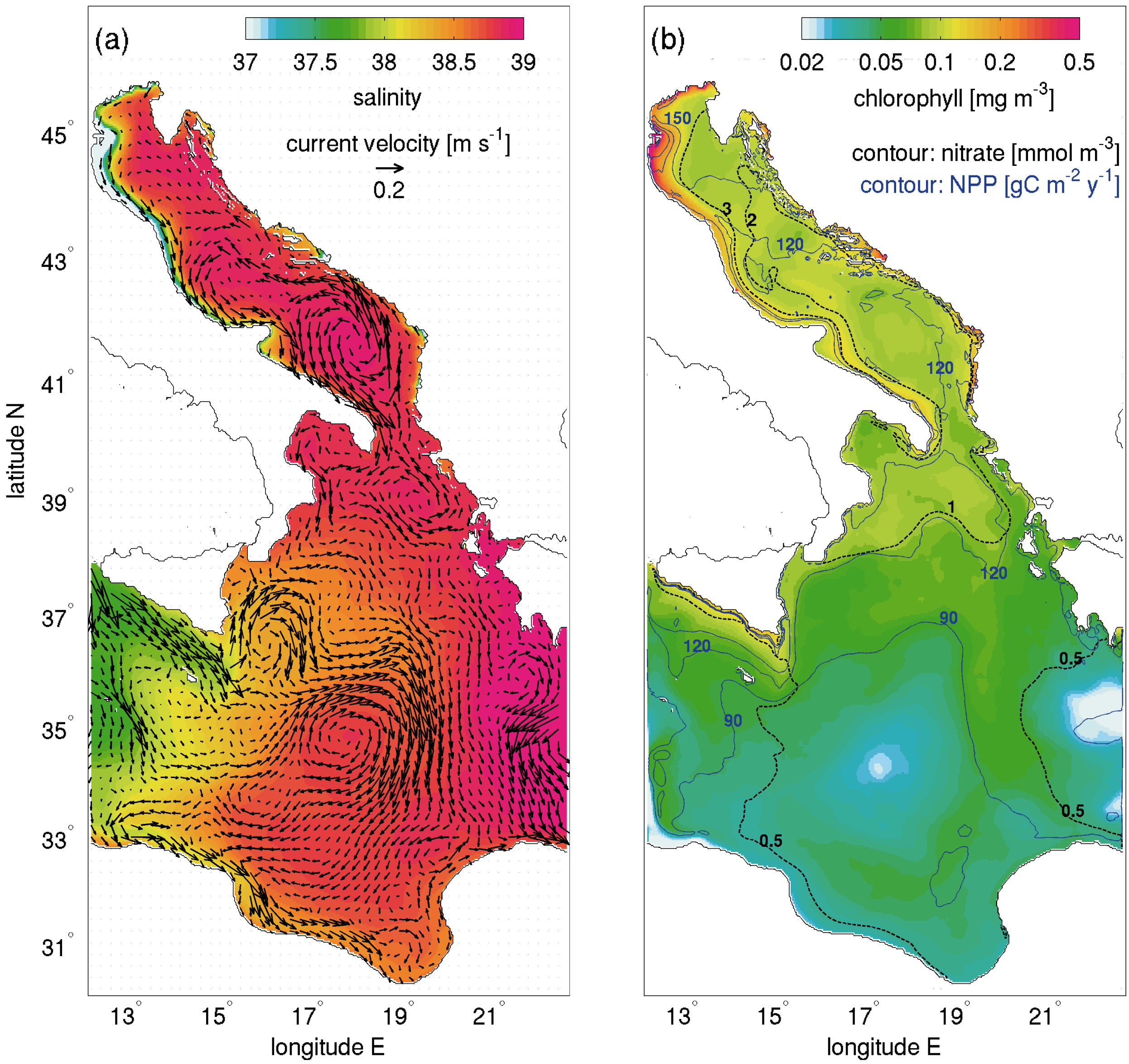

Figure 9: (a) Map of the surface currents (arrows) and salinity. (b) Map of the surface chlorophyll and contours (solid black lines) of nitrate concentration in the upper layer (0-20 m), and contours (dotted blue lines) of the annually averaged and vertically integrated (0-200 m) net primary production (NPP).

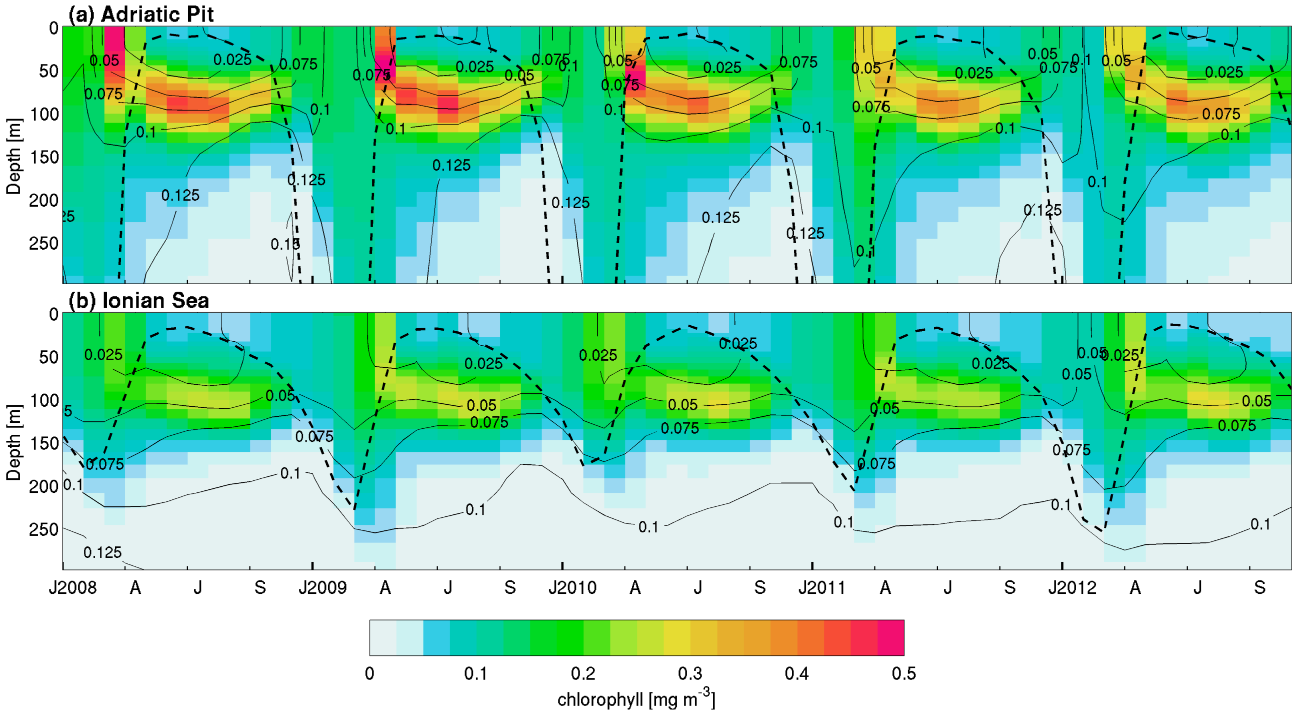

Figure 10: Hovmöller diagrams of chlorophyll (color) and phosphate (contour, [mmol m^{-3}]) and plots of the mixed layer depth (dashed lines, [m]) for the southern Adriatic Pit (a) and the Ionian offshore area (b).

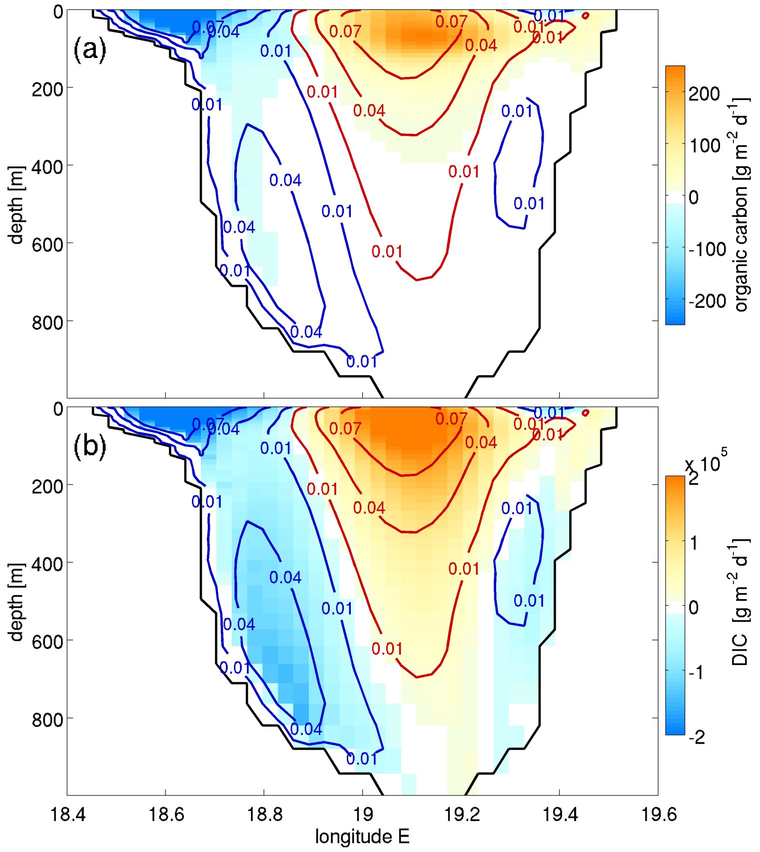

Figure 11: Fluxes of organic carbon (a) and DIC (b) across the Otranto Strait (dashed line in Fig. 8). The solid contours specify northward (red) and southward (blue) meridional velocities.

5

BFM name (Fig. 1)	Variable name	Unit	value	reference
$O^{(2)}$	oxygen	mmol m^{-3}	250	Saturation level in fresh water
$N^{(1)}$	phosphate	mmolP m^{-3}	2.6	Cossarini et al., 2015a, adapted from Ludwig et al., 2009
$N^{(3)}$	nitrate	mmol m^{-3}	150	Cossarini et al., 2015a, adapted from Ludwig et al., 2009
$N^{(4)}$	ammonio	mmol m^{-3}	34.1	Set equal to 1/5 of total nitrogen
$N^{(5)}$	silicate	mmol m^{-3}	150	Set equal to nitrate value
$O_c^{(3)}$	Dissolved Inorganic Carbon (DIC)	mg m^{-3}	33225	Cossarini et al., 2015b
$O^{(3)}$	Alkalinity	mmol m^{-3}	2800	Cossarini et al., 2015b

Table 1. Concentrations of tracers in the rivers.

LS_n	1 (Ref)	3	6	9	12
Δt_{trc} [s]	200	600	1200	1800	2400
Wallclock time [h] per 1-year simulation	65.8	29.5	17.3	14.5	15.1
Error of integrated 0-200m chlorophyll	0	0.01%	0.05%	0.1%	>10%

Table 2. Computational cost as a function of the longstep factor (LS_n) and the mean error of the integrated chlorophyll. The error was the annual average of the RMS of the differences between the longstep simulations and the reference (Ref) simulation. The error was normalized using the reference simulation.